

Multi-ethnic fine-mapping of 14 central adiposity loci

Ching-Ti Liu^{1,*}, Martin L. Buchkovich², Thomas W. Winkler³, Iris M. Heid^{3,4},
African Ancestry Anthropometry Genetics Consortium[†], GIANT Consortium[†],
Ingrid B. Borecki⁵, Caroline S. Fox⁶, Karen L. Mohlke², Kari E. North⁷ and L. Adrienne Cupples^{1,6,*}

¹Department of Biostatistics, Boston University, Boston, MA, USA, ²Department of Genetics, University of North Carolina at Chapel Hill, NC, USA, ³Department of Genetic Epidemiology, Institute of Epidemiology and Preventive Medicine, University of Regensburg, Regensburg, Germany, ⁴Institute of Epidemiology, Helmholtz Zentrum Muenchen-German Research Center for Environmental Health, Neuherberg, Germany, ⁵Division of Statistical Genomics, Department of Genetics, Washington University, St Louis, MO, USA, ⁶NHLBI Framingham Heart Study, Framingham, MA, USA and ⁷Department of Epidemiology and Carolina Population Center, Gillings School of Global Public Health, University of North Carolina, Chapel Hill, NC, USA

Received March 12, 2014; Revised April 15, 2014; Accepted April 16, 2014

The Genetic Investigation of Anthropometric Traits (GIANT) consortium identified 14 loci in European Ancestry (EA) individuals associated with waist-to-hip ratio (WHR) adjusted for body mass index. These loci are wide and narrowing the signals remains necessary. Twelve of 14 loci identified in GIANT EA samples retained strong associations with WHR in our joint EA/individuals of African Ancestry (AA) analysis (log-Bayes factor >6.1). Trans-ethnic analyses at five loci (*TBX15-WARS2*, *LYPLAL1*, *ADAMTS9*, *LY86* and *ITPR2-SSPM*) substantially narrowed the signals to smaller sets of variants, some of which are in regions that have evidence of regulatory activity. By leveraging varying linkage disequilibrium structures across different populations, single-nucleotide polymorphisms (SNPs) with strong signals and narrower credible sets from trans-ethnic meta-analysis of central obesity provide more precise localizations of potential functional variants and suggest a possible regulatory role. Meta-analysis results for WHR were obtained from 77 167 EA participants from GIANT and 23 564 AA participants from the African Ancestry Anthropometry Genetics Consortium. For fine mapping we interrogated SNPs within ± 250 kb flanking regions of 14 previously reported index SNPs from loci discovered in EA populations by performing trans-ethnic meta-analysis of results from the EA and AA meta-analyses. We applied a Bayesian approach that leverages allelic heterogeneity across populations to combine meta-analysis results and aids in fine-mapping shared variants at these locations. We annotated variants using information from the ENCODE Consortium and Roadmap Epigenomics Project to prioritize variants for possible functionality.

INTRODUCTION

Waist–hip ratio, a measure of body fat distribution, is associated with metabolic consequences independent of overall adiposity as measured by body mass index (BMI) (1–3). Evidence has indicated that body fat distribution is partially determined by genetic factors with age- and BMI-adjusted heritability estimates for waist–hip ratio ranging from 36–61% (4).

In the past few years, genome-wide association studies have seen numerous successes in the identification of genetic variants

associated with adiposity traits, including those characterizing centralized fat patterning. The Genetic Investigation of Anthropometric Traits (GIANT) consortium previously reported 14 loci associated with waist–hip ratio adjusted for BMI, age, age² and sex [waist-to-hip ratio (WHR)] in studies of European Ancestry (EA) (5). Recently, we also conducted a similar genome-wide association analysis in African Ancestry (AA) studies jointly from the African Ancestry Anthropometry Genetics (AAAG) Consortium, identifying one WHR-associated locus (6). While our analysis failed to detect genome-wide significant

*To whom correspondence should be addressed at: Department of Biostatistics, Boston University School of Public Health, 801 Massachusetts Ave, CT3, Boston, MA 02118, USA. Tel: +1 6176387752; Fax: +1 6176386484; Email: ctiu@bu.edu (C.-T.L.); Tel: +1 6176385176; Email: adrienne@bu.edu (L.A.C.)

[†]List of members are listed in the supplementary document.

Table 1. Trans-ethnic meta-analysis association results for 14 loci previously reported in EA sample

Loci information Genes	Index SNP ^a	chr	EA-sample only			Multi-ethnic meta-analysis results					
			LogBF ^b	Length ^c	<i>n</i> ^d	Lead SNP	LogBF ^c	Length ^c	<i>n</i> ^d	CEU LD ^f	YRI LD ^f
<i>TBX15-WARS2</i>	rs984222	1	12.68	27 654	4	rs984222	14.69	1591	3	Same	Same
<i>DNM3-PIGC</i>	rs1011731	1	8.95	54 037	11	rs9286854	10.01	48 775	10	0.9 (1.0)	0.5 (0.8)
<i>LYPLAL1</i>	rs4846567	1	10.28	14 8141	23	rs2820443	11.84	27 409	8	1.0 (1.0)	0.9 (1.0)
<i>GRB14</i>	rs10195252	2	8.60	31 272	4	rs1128249	12.10	31 272	5	0.9 (1.0)	1.0 (1.0)
<i>NISCH-STAB1</i>	rs6784615	3	5.83	27 7969	10	rs6784615	5.61	43 1135	10	Same	Same
<i>ADAMTS9</i>	rs6795735	3	5.78	30 676	13	rs4132228	8.48	8669	7	0.4 (1.0)	0.1 (1.0)
<i>CPEB4</i>	rs6861681	5	5.03	93 159	11	rs10516107	5.47	93 159	12	1.0 (1.0)	N/A
<i>LY86</i>	rs1294421	6	7.41	15 862	6	rs1294410	9.89	6952	5	0.8 (1.0)	0.4 (0.7)
<i>VEGFA</i>	rs6905288	6	8.43	5678	2	rs1358980	10.83	6655	2	0.6 (0.9)	0.1 (1.0)
<i>RSPO3</i>	rs9491696	6	12.89	66 820	33	rs7766106	16.42	60 186	20	1.0 (1.0)	0.8 (0.9)
<i>NFE2L3</i>	rs1055144	7	7.03	38 160	13	rs4141278	6.91	36 707	10	1.0 (1.0)	0.0 (1.0)
<i>ITPR2-SSPN</i>	rs718314	12	6.96	38 192	13	rs7302344	8.25	28 393	8	0.6 (0.9)	0.1 (1.0)
<i>HOXC13</i>	rs1443512	12	6.71	7447	3	rs1443512	7.27	7447	3	Same	Same
<i>ZNRF3-KREMEN1</i>	rs4823006	22	6.55	2194	3	rs4823006	6.84	2194	2	Same	Same

^aTop variants identified in Heid *et al.* (2010) (5).

^bEvidence of association for the index SNP in EA-sample only.

^cLength of 95% credible region in base pair.

^dThe number of SNPs of interest, potential causal or tagging to the causal, within the region.

^eEvidence of association for the lead SNP in EA + AA sample.

^fLD information, r^2 (D'), between the index SNP and the lead SNP.

association findings overlapping those in the GIANT Consortium, our lead single-nucleotide polymorphism (SNP) rs6931262 at newly identified *RREB1* in AA is 474 kb away from the lead SNP rs1294421 at *LY86* in EA. Given the low pairwise linkage disequilibrium (LD), these variants likely represent two independent signals. However, they may be also partially tagging an untyped functional variant that contributes to both underlying associations. In addition, 12 of 14 SNPs had the same effect direction with respect to the beta coefficient (P -value = 0.0065) between AA and EA samples and five index SNPs in EA demonstrated nominal significance (P -value < 0.05) in AA. These results may demonstrate similarity in the genetic architecture in EA and AA and suggests that trans-ethnic association analysis may provide further information in fine-mapping the previously identified loci.

Most previous genome-wide association studies (GWAS) have been conducted separately by race/ethnicity due to concerns with allelic heterogeneity and differing patterns of LD between populations. In the present study, we use a Bayesian approach to exploit precisely these differences between EA and AA samples to fine map variants at WHR loci first identified in EA samples.

RESULTS

MANTRA results of 14 previously identified GIANT loci

Twelve of 14 previously published loci (index SNP) in the samples of EA retained strong evidence for association (logBF > 6.1) with WHR in the joint trans-ethnic analysis of EA and AA samples (Table 1). We used a stringent threshold, i.e. logBF value of at least 6.1 based on empirical simulation results reported by Wang *et al.* (7), which most closely approximates genome-wide significance. None of the 14 loci displayed heterogeneity in their allelic effects (all posterior probabilities for heterogeneity < 0.95). At four loci, the originally reported

associated SNP remained the lead SNP for that region (i.e. the SNP with the largest logBF within each locus): rs984222 at *TBX15-WARS2*; rs6784615 at *NISCH-STAB1*; rs1443512 at *HOXC13*; and rs4823006 at *ZNRF3-KREMEN1*. For the remaining 10 loci, different SNPs with greater effect sizes and reduced credible regions were identified; all alternate SNPs are in LD with the previously identified variants in EA ($r^2 > 0.4$ in HapMap II CEU).

We constructed 95% credible sets (CSs) for the meta-analysis results from GIANT EA samples only and for the trans-ethnic meta-analysis result (Table 1). Eight of the 95% CSs obtained from trans-ethnic association analyses generated shorter CSs length ranging from 4 to 94% length reduction (*DNM3-PIGC*, *NFE2L3*, *LY86*, *LYPLAL1*, *ADAMTS9*, *ITPR2-SSPN*, *RSPO3* and *TBX15-WARS2*) compared with the sets based on EA samples only (Fig. 1 and Supplementary Material, Fig. S1) and five (*LY86*, *LYPLAL1*, *ADAMTS9*, *ITPR2-SSPN* and *TBX15-WARS2*) of them have >25% length reduction. The greatest decrease in the distance spanned by the 95% CS of SNPs was at the locus *LYPLAL1*, where the CS was reduced by ~80% from 148 141 bp in the analysis of EA samples only to 27 409 bp in the trans-ethnic analysis (Fig. 1A). The LD surrounding the original index SNP in this locus is much stronger in CEU compared with that in YRI. In addition, a few SNPs in high LD with the index SNP in both populations have enhanced association signals and the LD block with the index SNP is much narrower in YRI samples, leading to a much narrower CS in trans-ethnic analysis and dropping 15 variants from EA-derived CS. The distance spanned by SNPs at the locus *ADAMTS9* decreased 72% from 30 679 to 8669 bp by comparing trans-ethnic analysis to the EA sample only analysis (Fig. 1B). Neither CEU nor YRI have strong LD with many variants surrounding the original index SNPs; however, the variants in strong LD with the index SNP are within a narrow region in both samples of ancestries (narrower in YRI than in CEU). The association signals are highly enhanced and association

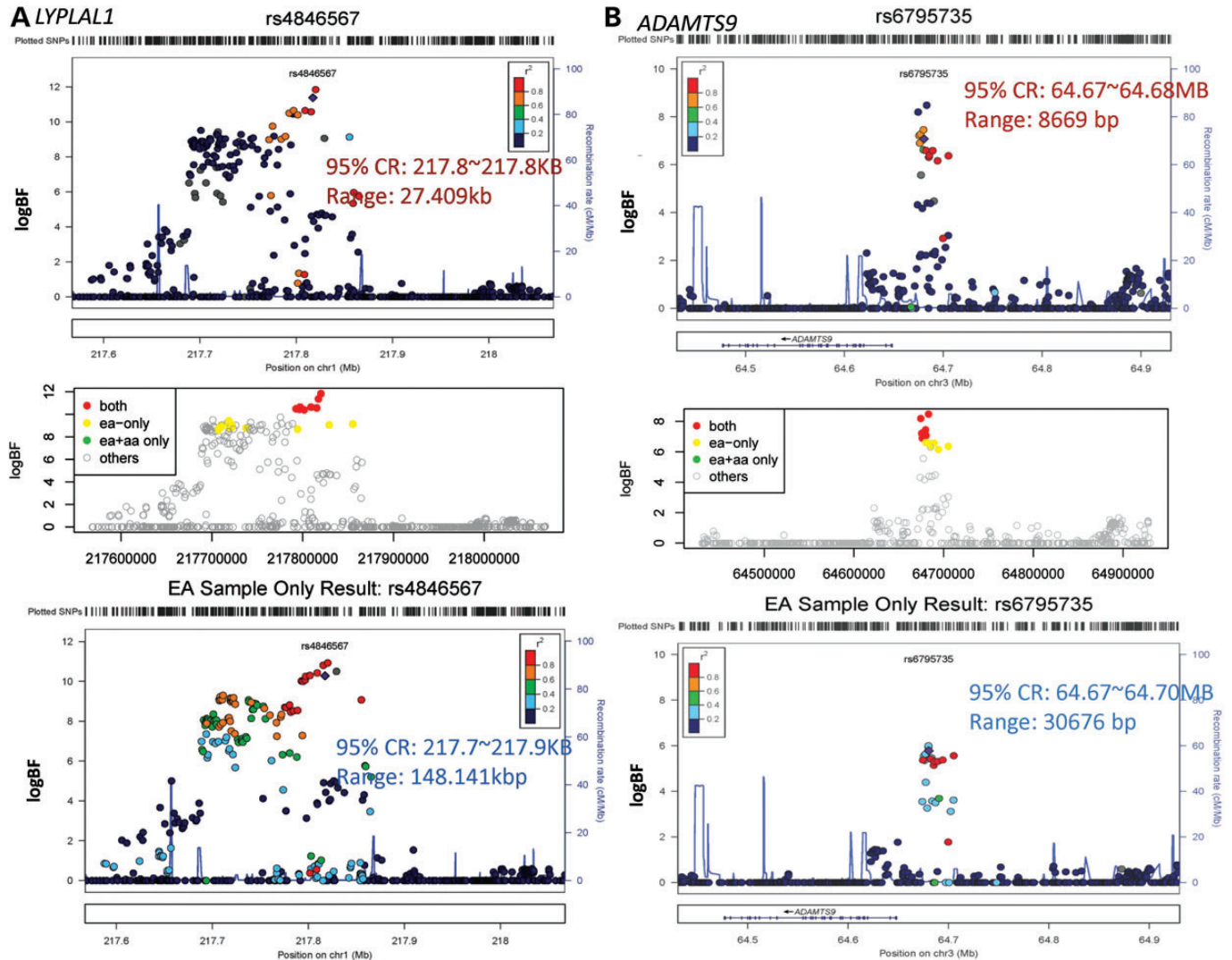


Figure 1. Regional plot of loci *LYPLAL1* and *ADAMTS9*. The top panel is obtained from the trans-ethnic meta-analysis result with HapMAP II YRI LD information. The middle panel classifies variants based on whether they are included in the none, either or both of CSs. The red points represent variants retained in both credible regions constructed using EA and trans-ethnic samples; yellow and green points represent variants retained in CSs constructed using EA and trans-ethnic samples, separately; the gray points represents variants which do not fall in any CS. The bottom panel is from EA sample only analysis with HapMap II CEU linkage disequilibrium information. **(A)** Regional plot of loci *LYPLAL1* (Chr1:217 413 815–217 452 830). There are eight SNPs commonly shared by the CSs obtained from EA-only and EA + AA. Fifteen additional SNPs are included in the EA-only derived CS while no additional SNP is included in the EA + AA-derived CS. The length change from 148 141 to 27 409 bp for EA-only and EA + AA derived CSs, respectively. The LD surrounding the original index SNP is much stronger in CEU compared with that in YRI. In addition, few SNPs with high LD with the index SNP in both populations have enhanced association signals and the LD block with the index SNP is much narrower in YRI samples, leading to a much narrower CS in trans-ethnic analysis and dropping 15 variants from EA-derived CS. **(B)** Regional plot of loci *ADAMTS9* (Chr3:64 575 591–64 648 405). There are 7 SNPs commonly shared by the CSs obtained from EA-only and EA + AA. Six additional SNPs are included in the EA-only derived CS while no additional SNP is included in the EA + AA-derived CS. The length change from 30 676 to 8669 bp for EA-only and EA + AA derived CSs, respectively. Neither CEU nor YRI have strong LD for many variants surrounding the original index SNPs; however, the variants with strong LD with index SNP are within a narrow region in both samples of ancestries (narrower in YRI than in CEU). The association signals are highly enhanced and association signals for those top variants are more distinguishable in trans-ethnic analysis compared with EA sample only analysis. These lead to the dropping of six variants from EA-derived CS to form a more compact and narrower trans-ethnic analysis derived CS.

signals for those top variants are more distinguishable in trans-ethnic analysis compared with EA sample only analysis. This result leads to dropping six variants from EA-derived CS to form a more compact and narrower trans-ethnic-derived CS. Compared with EA results, 4 of 14 CSs (*GRB14*, *CPEB4*, *HOXC13* and *ZNRF3-KREMEN1*) remain the same length, and 2 of 14 loci (*NISCH-STAB1* and *VEGFA*) had longer credible regions. Among these six loci, only one CS

(*NISCH-STAB1*) has a substantial increase in the length of credible regions (Supplementary Material, Fig. S1). At this locus there is very weak LD surrounding the original index SNP in EA sample. In addition, the signals for the index SNP and most variants in the region are weak in both EA and AA samples and the trans-ethnic analysis does not enhance the association signals ($\log_{10}BF < 6.1$). Therefore, the CS in this case may not be informative.

Table 2. CS SNPs overlapping evidence of regulatory elements

CS SNPs Loci/SNP	Chr	Position	Nearest coding TSS	Regulatory datasets overlapping SNPs (by tissue)							
				<i>N</i> ^a	Open chromatin ^b	H3K4me1	H3K27ac	H3K4me3	H3K9ac	H3K4me2	
<i>TBX15-WARS2</i>											
rs984222	1	119 503 843	26 585	<i>TBX15</i>	19		AOMLB	AOML	OL	L	OL
rs984225	1	119 504 284	26 144	<i>TBX15</i>	16		AOML	AOML	OL	L	OL
rs10923712	1	119 505 434	24 994	<i>TBX15</i>	10		AOML	AOML		L	
<i>LYPLAL1</i>											
rs1415293	1	219 730 006	371 938	<i>SLC30A10</i>	4		ON	ON			
rs2820446	1	219 748 818	353 126	<i>SLC30A10</i>	3	B	B				B
<i>ADAMTS9</i>											
rs4504165	3	64 701 890	-28 214	<i>ADAMTS9</i>	4			AM		M	
<i>LY86</i>											
rs912056	6	6 736 197	147 270	<i>LY86</i>	5		AM	M		M	
rs1294407	6	6 738 103	149 176	<i>LY86</i>	14		AOM	AM	AOM		OME
rs1294409	6	6 738 355	149 428	<i>LY86</i>	9		AM	A	AOM		OM
<i>ITPR2-SSPN</i>											
rs7132434	12	26 472 562	123 957	<i>SSPN</i>	23	MNILB	AOMNELB	AOMN		M	OML
rs1049376	12	26 491 475	142 870	<i>SSPN</i>	14		MNE	MN	N	MN	M

For loci with >25% decrease in CS size, CS SNPs overlapping two or more regulatory datasets in the same tissue are shown. Negative distance from nearest GENCODE v12 basic annotation TSS indicates the variant is downstream of the TSS relative to the direction of transcription. Tissues with elements overlapping each SNP are indicated as A, adipose; B, blood; E, endothelial; I, pancreatic islets; L, liver; M, muscle; N, brain; O, bone; Chr, chromosome; TSS, transcription start site.

^aNumber indicates the total number of overlapping datasets across experiments and cell types.

^bOverlap with FAIRE and/or DNaseI hypersensitivity elements indicates open chromatin.

Bioinformatic annotations for the SNPs in CSs

To evaluate the regulatory potential of the CS SNPs at the five loci with the greatest decrease (>25%) in CS length, we examined whether these SNPs map within candidate regulatory elements identified by the ENCODE Consortium and Roadmap Epigenomics Project. We analyzed regulatory elements defined as experimentally detected regions of open chromatin, histone modification enrichment, and transcription factor binding in tissues (blood, brain, endothelial, liver, muscle and pancreatic islet in ENCODE Consortium; adipose, brain, liver, muscle and pancreatic islet in Roadmap Epigenomics Project) that we hypothesize may play a role in WHR pathways (Supplementary Material, Table S1). In total, 11 of the 32 (34.4%) CS SNPs at these loci overlapped elements in two or more datasets in the same tissue, suggesting that they are located in regions with evidence of regulatory activity. The SNPs overlapped regulatory elements from an average of 11 datasets and a maximum of 23 datasets.

Two SNPs at *LYPLAL1* are located in regions with evidence of regulatory activity in distinct tissues (Table 2). While rs1415293 maps within regulatory elements in bone and neuronal tissues, rs2820446 is in a region of regulatory elements in blood (Fig. 2). At the *TBX15-WARS2* locus we identified three SNPs within a 1.6 kb region with strong evidence of regulatory activity in adipose, bone, muscle and liver tissues (Table 2). At *ITPR2-SSPN*, rs7132434 overlaps the largest number (23) of regulatory element datasets.

We also examined variants in LD ($r^2 > 0.8$) with any of the thirty-two 95% CS SNPs in either the European (EUR) or African (AFR) 1000 Genomes samples. Ten additional variants overlap regions with evidence of regulatory activity (Supplementary Material, Table S2), usually from the same tissues as the CS SNPs at the locus.

DISCUSSION

We performed association analysis of WHR at 14 previously published loci via trans-ethnic meta-analysis. Among the 14 loci, 9 of the 95% CSs obtained from trans-ethnic association studies contained fewer SNPs. Additionally, the trans-ethnic association studies shortened the length of the 95% credible regions for eight loci, and five of them shortened the length >25%: *TBX15-WARS2* (from 27 654 to 1591 bp), *ADAMTS9* (from 30 676 to 8669 bp), *LY86* (from 15 862 to 6952 bp), *LYPLAL1* (from 148 141 to 27 409 bp) and *ITPR2-SSPN* (from 38 192 to 28 393 bp).

We observed that several of the loci had a different lead SNP in the trans-ethnic results compared with the EA only result. It is likely that when a signal is very strong in a locus and there are few variants in the locus that are in high LD, the lead SNP in trans-ethnic analysis will remain the same. An explanation for the lead SNP changing is LD differences between EA and AA samples. The best functional variant-tagged SNP may differ due to the varying LD structure across different populations and the trans-ethnic meta-analysis accounts for allelic heterogeneity that may lead to a different strongest associated SNP. In addition, the association evidence for a newly identified best SNP is often not much different from the evidence of original index SNP, so random fluctuation may also contribute to the lead SNP changing.

The structure of LD and the strength of signals within each locus likely influence the length of a CS. We observe that some CSs become substantially reduced in size in trans-ethnic meta-analysis results compared their counterpart in EA-only meta-analysis in the loci such as *LYPLAL1*, *ADAMTS9* and *LY86*. These loci share similar patterns in that there is a strong signal in the EA sample and the signal becomes enhanced in the multi-ethnic meta-analysis. In addition, the LD is weaker

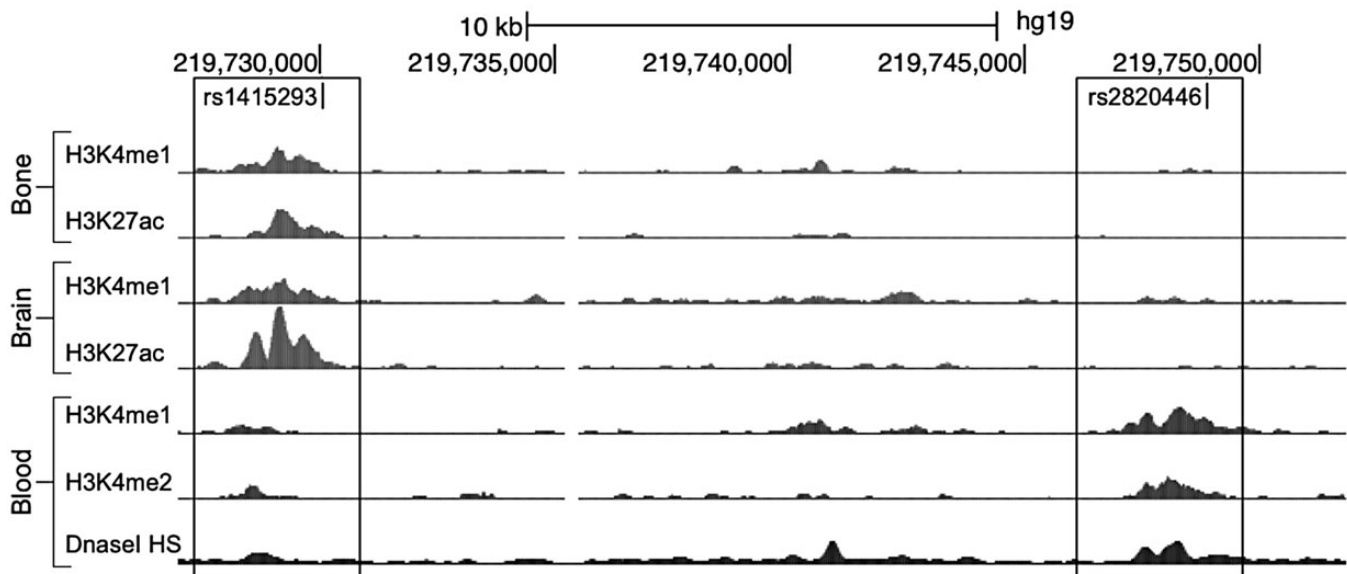


Figure 2. CS SNPs at *LYPLALI* in regions with evidence of regulatory activity in distinct tissues UCSC genome browser signal enrichment tracks from regulatory datasets with elements overlapping rs1415293 (left-most box; bone and brain) and rs2820446 (right-most box; blood) are shown.

in the AA sample within these loci, thus highlighting several top variants. These properties lead to reduced CSs in trans-ethnic meta-analysis. On the other hand, some loci do not have a strong enough signal in the EA sample and weak LD pattern within the locus, such as *NISCH-STAB1*, leading to uninformative CSs (Supplementary Material, Fig. S1).

Many genetic association signals are shared across populations. Ioannidis *et al.* (8) demonstrated that for common variants, the magnitude of effect estimates was similar across racial groups; however, allele frequencies varied across racial groups, resulting in differences in the power to detect effects across populations. Several studies examining a range of traits have reported the transferability of disease susceptible genetic loci across different race/ethnic populations (6,9,10). There have been several trans-ethnic analyses reported (11–13); however, there is no analysis, to our knowledge, reporting on the genetic associations for central adiposity by jointly analyzing data from different race/ethnic populations simultaneously. Therefore, assuming that there is a shared signal across populations, our analysis employing MANTRA offers additional insight to uncover the genetic architecture for WHR by taking advantage of results from different race/ethnic groups.

Examining overlap with regulatory elements narrowed a list of 86 candidate SNPs at five loci to 21 SNPs that may influence transcription in WHR relevant cell lines and tissues. *LYPLALI* SNPs overlap two regions with evidence of regulatory activity in different tissues, suggesting that SNPs in these regions may have distinct influences on transcription in different tissues. Further testing is needed to identify whether these variants influence transcriptional activity in these cell types. We also identified a 1.6 kb region near *TBX15-WARS2* with evidence of regulatory activity in multiple tissues including adipose tissue. One SNP in this region, rs984222, has been previously reported to have *cis*-regulatory effects on *TBX15* transcription in omental adipose tissue (5), further supporting the plausibility that this or

another nearby SNP may influence transcriptional activity. A region near the transcription start site (<100 bp) of the lncRNA, RP11-513G19.1, overlaps more regulatory elements than any other CS SNP evaluated and has strong evidence of enhancer activity in most of the tissues tested. The epigenomic data do not distinguish whether this candidate regulatory element influences transcription of the lncRNA, or a more distal gene such as *ITPR2* or *SSPN*. Further studies are needed to elucidate the regulatory effect of these SNPs on nearby transcripts and their connections to WHR biology.

This analysis identifies CS SNPs overlapping regions with evidence of regulatory activity that suggest good candidates for follow-up studies and also provides insight into the possible tissues in which these variants may regulate transcription. Including additional regulatory datasets from these or other tissues may identify additional candidate regulatory variants and target tissues.

In summary, we performed a trans-ethnic meta-analysis for WHR with previously published EA and AA meta-analysis results using an analytical approach, MANTRA, which allowed for different underlying allelic effects between race/ethnic groups. As the genomic regions harboring genetic signals that were shared across the different race/ethnic populations were more likely to contain functional variants, we gained power by incorporating all the samples together, at least for those loci that generalized across population groups. This approach is especially applicable to the analysis of samples of AA, since more limited LD is observed in these populations, aiding in fine-mapping. Our results may have been limited by the fact that our EA sample size was much larger than our AA sample size. Indeed, the effects of this difference in sample size require further investigation. Overall, in leveraging varying LD structures across different populations, SNPs with the strongest signals and the CSs from our trans-ethnic meta-analysis provide more precise localization of variants for future functional analysis.

MATERIALS AND METHODS

Design and samples

We conducted a meta-analysis of summary results from EA and AA GWAS. For the EA data, we used meta-analysis association results from up to 77 167 individuals in 32 cohorts, published by the GIANT consortium (5). For the AA data, we used the meta-analysis GWAS results from up to 19 744 individuals in 14 cohorts in the AAAG Consortium (6). For both EA and AA data, we obtained the results from the fixed-effects and inverse variance-weighted meta-analyses of study-specific association analyses. In this paper, we focused on the 14 loci (*TBX15-WARS2*, *DNM3-PIGC*, *LYPLAL1*, *GRB14*, *NISCH-STAB1*, *ADAMTS9*, *CPEB4*, *LY86*, *VEGFA*, *RSPO3*, *NFE2L3*, *ITPR2-SSPN*, *HOXC13*, *ZNRF3-KREMEN1*) previously identified in the participants of EA in GIANT (5).

Phenotypes

We analyzed the association of WHR, a measure of body fat distribution. For both the GIANT consortium and the AAAG Consortium, each cohort created residuals for WHR adjusted for age, age², study site (if applicable) and BMI. The residuals were inverse normal transformed and then used as the phenotypes in association analysis within each participating cohort. Each participating cohort used principal components as needed in regression models assessing the association of a SNP to account for population stratification. Details regarding the trait creation and participating studies can be found in the original publications (5,6).

Statistical analysis

We meta-analyzed the two sets of results for the 14 previously reported loci with MANTRA software (Meta-Analysis of Trans-ethnic Association studies) (14). MANTRA is a meta-analysis approach that can be used to combine GWAS results from more than one ancestry based on the expectation of similar allelic effects between the most closely related populations (14). Technically, populations are clustered based on the average allele frequency difference by means of a Bayesian partition model and populations within the same cluster are assumed to have the same underlying allelic effect while allowing heterogeneity for populations in different clusters. The evidence in favor of association of the trait with the genetic variant is quantified with a Bayes' factor (BF) and a log₁₀ BF of 6.1 or higher is approximately comparable to a genome-wide significance threshold of $P < 5 \times 10^{-8}$ (7). Specifically in our application, we conduct the fixed-effect meta-analysis within each race assuming there is no genetic heterogeneity across the samples of participating cohorts from the same race. Then, we implemented MANTRA to meta-analyze the association results from EA and AA samples.

Construction of 95% CSs

We used MANTRA results to construct a fine-mapping interval for each associated index variant (13). We constructed these intervals from analysis in the EA only set (GIANT results) and in the results from the trans-ethnic analysis. To create a 95% CS, we analyzed variants within 250 kb upstream and

downstream from the variant with the index SNP. The algorithm to construct a CS is the following:

- (1) As described in MANTRA, obtain the BF value for each variant in the region.
- (2) For each SNP_{*j*}, calculate the posterior probability that the SNP is driving the association signal within the region, i.e. BF_{*j*} divided by summation of BF over all SNPs within the region.
- (3) Rank all SNPs within the region according to their BFs, such that BF_(*i*) represents the *i*th largest BF.
- (4) Proceed down the ranked list until the accumulative posterior probability exceeds 95% of the total cumulative posterior probably for all SNPs in the locus.
- (5) Include in the 95% CS those SNPs with accumulative posterior probability of 0.95. We define the length associated with each CS as the length of the region in base pairs spanned by the SNPs retained in the specific CS.

Bioinformatics annotation

We annotated variants in the 95% CSs at the five loci that displayed a >25% decrease in 95% CS kilobase size in trans-ethnic analysis compared with the analysis in EA only: *ADAMTS9*, *TBX15-WARS2*, *LYLPAL1*, *ITPR2-SSPN* and *LY86*. Although the 25% decrease is an arbitrary cutoff, we chose it to focus on those CSs where there was a substantial decrease, suggesting that trans-ethnic analyses aided in fine mapping. To identify SNPs that may contribute to an association signal but were not tested in the MANTRA analysis, we also identified SNPs in strong LD with the 95% CS SNPs in either EA or AA ($r^2 > 0.8$, AFR or EUR 1000 Genomes Phase1 version 2 release) (15). None of the interrogated variants are coding variants. The distance from each tested SNP to the nearest transcription start site of a coding gene was calculated using basic transcript annotation from GENCODE version 12 (16).

To examine variant overlap with elements from regulatory datasets, we downloaded data for selected tissue and cell types describing the locations of regions of open chromatin (DNase-seq, FAIRE-seq), histone modification signal enrichment (H3K4me1, H3K27ac, H3K4me3, H3K9ac and H3K4me2), and transcription factor binding generated by the ENCODE Consortium (17) and Roadmap Epigenomics Project (18). Data from the ENCODE Integrative Analysis were used when available (19). For consistency in processing the data across consortia, we downloaded sequence alignments from the Roadmap Epigenomics project and identified regions of enrichment using the same irreproducible discovery rate (20) pipeline as ENCODE. For tissues with only one replicate, we used only MACS2 (21) to identify regions of signal enrichment. A total of 224 datasets were collected for this analysis (Supplementary Material, Table S1).

SUPPLEMENTARY MATERIAL

Supplementary Material is available at *HMG* online.

ACKNOWLEDGEMENTS

We would like to thank Andrew Morris's kindness in providing the MANTRA package and discussion.

Conflict of Interest statement. None declared.

FUNDING

This work is partially supported by grant NGFNPLUS 01GS0823 (T.W.W. and I.M.H.), National Institutes of Health (NIH) R01DK8925601 (I.B.B., L.A.C. and C.T.L.), R01DK072193 (K.L.M.), R21DA027040 (K.L.M.), T32GM067553 (M.L.B.) and American Heart Association 13PRE16930025 (M.L.B.).

REFERENCES

- Carey, V.J., Walters, E.E., Colditz, G.A., Solomon, C.G., Willett, W.C., Rosner, B.A., Speizer, F.E. and Manson, J.E. (1997) Body fat distribution and risk of non-insulin-dependent diabetes mellitus in women. The Nurses' Health Study. *Am. J. Epidemiol.*, **145**, 614–619.
- Lindgren, C.M., Heid, I.M., Randall, J.C., Lamina, C., Steinthorsdottir, V., Qi, L., Speliotes, E.K., Thorleifsson, G., Willer, C.J., Herrera, B.M. *et al.* (2009) Genome-wide association scan meta-analysis identifies three loci influencing adiposity and fat distribution. *PLoS Genet.*, **5**, e1000508.
- Wang, Y., Rimm, E.B., Stampfer, M.J., Willett, W.C. and Hu, F.B. (2005) Comparison of abdominal adiposity and overall obesity in predicting risk of type 2 diabetes among men. *Am. J. Clin. Nutr.*, **81**, 555–563.
- Rose, K.M., Newman, B., Mayer-Davis, E.J. and Selby, J.V. (1998) Genetic and behavioral determinants of waist–hip ratio and waist circumference in women twins. *Obes. Res.*, **6**, 383–392.
- Heid, I.M., Jackson, A.U., Randall, J.C., Winkler, T.W., Qi, L., Steinthorsdottir, V., Thorleifsson, G., Zillikens, M.C., Speliotes, E.K., Mägi, R. *et al.* (2010) Meta-analysis identifies 13 new loci associated with waist–hip ratio and reveals sexual dimorphism in the genetic basis of fat distribution. *Nat. Genet.*, **42**, 949–960.
- Liu, C.T., Monda, K.L., Taylor, K.C., Lange, L., Demerath, E.W., Palmas, W., Wojczynski, M.K., Ellis, J.C., Vitolins, M.Z., Liu, S. *et al.* (2013) Genome-wide association of body fat distribution in African ancestry populations suggests new loci. *PLoS Genet.*, **9**, e1003681.
- Wang, X., Chua, H.X., Chen, P., Ong, R.T., Sim, X., Zhang, W., Takeuchi, F., Liu, X., Khor, C.C., Tay, W.T. *et al.* (2013) Comparing methods for performing trans-ethnic meta-analysis of genome-wide association studies. *Hum. Mol. Genet.*, **22**, 2303–2311.
- Ioannidis, J.P., Ntzani, E.E. and Trikalinos, T.A. (2004) 'Racial' differences in genetic effects for complex diseases. *Nat. Genet.*, **36**, 1312–1318.
- Liu, C.T., Garnaas, M.K., Tin, A., Kottgen, A., Franceschini, N., Peralta, C.A., de Boer, I.H., Lu, X., Atkinson, E., Ding, J. *et al.* (2011) Genetic association for renal traits among participants of African ancestry reveals new loci for renal function. *PLoS Genet.*, **7**, e1002264.
- Liu, C.T., Ng, M.C., Rybin, D., Adeyemo, A., Bielinski, S.J., Boerwinkle, E., Borecki, I., Cade, B., Chen, Y.D., Djousse, L. *et al.* (2012) Transferability and fine-mapping of glucose and insulin quantitative trait loci across populations: CARE, the Candidate Gene Association Resource. *Diabetologia*, **55**, 2970–2984.
- Rosenberg, N.A., Huang, L., Jewett, E.M., Szpiech, Z.A., Jankovic, I. and Boehnke, M. (2010) Genome-wide association studies in diverse populations. *Nat. Rev. Genet.*, **11**, 356–366.
- Dastani, Z., Hivert, M.F., Timpson, N., Perry, J.R., Yuan, X., Scott, R.A., Henneman, P., Heid, I.M., Kizer, J.R., Lytykäinen, L.P. *et al.* (2012) Novel loci for adiponectin levels and their influence on type 2 diabetes and metabolic traits: a multi-ethnic meta-analysis of 45,891 individuals. *PLoS Genet.*, **8**, e1002607.
- Franceschini, N., van Rooij, F.J., Prins, B.P., Feitosa, M.F., Karakas, M., Eckfeldt, J.H., Folsom, A.R., Kopp, J., Vaez, A., Andrews, J.S. *et al.* (2012) Discovery and fine mapping of serum protein loci through transethnic meta-analysis. *Am. J. Hum. Genet.*, **91**, 744–753.
- Morris, A.P. (2011) Transethnic meta-analysis of genomewide association studies. *Genet. Epidemiol.*, **35**, 809–822.
- Abecasis, G.R., Auton, A., Brooks, L.D., DePristo, M.A., Durbin, R.M., Handsaker, R.E., Kang, H.M., Marth, G.T., McVean, G.A. and Consortium, G.P. (2012) An integrated map of genetic variation from 1,092 human genomes. *Nature*, **491**, 56–65.
- Harrow, J., Frankish, A., Gonzalez, J.M., Tapanari, E., Diekhans, M., Kokocinski, F., Aken, B.L., Barrell, D., Zadissa, A., Searle, S. *et al.* (2012) GENCODE: the reference human genome annotation for The ENCODE Project. *Genome Res.*, **22**, 1760–1774.
- Consortium, E.P. (2011) A user's guide to the encyclopedia of DNA elements (ENCODE). *PLoS Biol.*, **9**, e1001046.
- Bernstein, B.E., Stamatoyannopoulos, J.A., Costello, J.F., Ren, B., Milosavljevic, A., Meissner, A., Kellis, M., Marra, M.A., Beaudet, A.L., Ecker, J.R. *et al.* (2010) The NIH Roadmap Epigenomics Mapping Consortium. *Nat. Biotechnol.*, **28**, 1045–1048.
- Dunham, I., Kundaje, A., Aldred, S.F., Collins, P.J., Davis, C.A., Doyle, F., Epstein, C.B., Frietze, S., Harrow, J., Kaul, R. *et al.* (2012) An integrated encyclopedia of DNA elements in the human genome. *Nature*, **489**, 57–74.
- Li, Q., Brown, J.B., Huang, H. and Bickel, P.J. (2011) Measuring reproducibility of high-throughput experiments. *Ann. Appl. Stat.*, **5**, 1752–1779.
- Feng, J., Liu, T., Qin, B., Zhang, Y. and Liu, X.S. (2012) Identifying ChIP-seq enrichment using MACS. *Nat. Protoc.*, **7**, 1728–1740.

Supplementary Document

African Ancestry Anthropometry Genetics Consortium

§ The members in **African Ancestry Anthropometry Genetics Consortium** include Ching-Ti Liu, Keri L. Monda, Kira C Taylor, Leslie Lange, Ellen W. Demerath, Walter Palmas, Mary K. Wojczynski, Jaclyn C. Ellis, Mara Z. Vitolins, Simin Liu, George J. Papanicolaou, Marguerite R. Irvin, Luting Xue, Paula J. Griffin, Michael A. Nalls, Adebowale Adeyemo, Jiankang Liu, Guo Li, Edward A. Ruiz-Narvaez, Wei-Min Chen, Fang Chen, Brian E. Henderson, Robert C. Millikan, Christine B. Ambrosone, Sara S. Strom, Xiuqing Guo, Jeanette S. Andrews, Yan V. Sun, Thomas H. Mosley, Lisa R. Yanek, Daniel Shriner, Talin Haritunians, Jerome I. Rotter, Elizabeth K. Speliotes, Megan Smith, Lynn Rosenberg, Josyf Mychaleckyj, Uma Nayak, Ida Spruill, W. Timothy Garvey, Curtis Pettaway, Sarah Nyante, Elisa V. Bandera, Angela F. Britton, Alan B. Zonderman, Laura J. Rasmussen-Torvik, Yii-Der Ida Chen, Jingzhong Ding, Kurt Lohman, Stephen B. Kritchevsky, Wei Zhao, Patricia A. Peyser, Sharon L.R. Kardia, Edmond Kabagambe, Ulrich Broeckel, Guanjie Chen, Jie Zhou, Sylvia Wassertheil-Smoller, Marian L. Neuhouser, Evadnie Rampersaud, Bruce Psaty, Charles Kooperberg, JoAnn E. Manson, Lewis H. Kuller, Heather M. Ochs-Balcom, Karen C. Johnson, Lara Sucheston, Jose M. Ordovas, Julie R. Palmer, Christopher A. Haiman, Barbara McKnight, Barbara V. Howard, Diane M. Becker, Lawrence F. Bielak, Yongmei Liu, Matthew A Allison, Struan F.A. Grant, Gregory L. Burke, Sanjay R. Patel, Pamela J. Schreiner, Ingrid B. Borecki, Michele K. Evans, Herman Taylor, Michele M Sale, Virginia Howard, Christopher S Carlson, Charles N. Rotimi, Mary Cushman, Tamara B. Harris, Alexander P Reiner, L. Adrienne Cupples, Kari E. North, Caroline S. Fox

GIANT Consortium

¥ The members in **GIANT Consortium** include Iris M Heid, Anne U Jackson, Joshua C Randall, Thomas W Winkler, Lu Qi, Valgerdur Steinthorsdottir, Gudmar Thorleifsson, M Carola Zillikens, Elizabeth K Speliotes, Reedik Mägi, Tsegaselassie Workalemahu, Charles C White, Nabila Bouatia-Naji, Tamara B Harris, Sonja I Berndt, Erik Ingelsson, Cristen J Willer, Michael N Weedon, Jian'an Luan, Sailaja Vedantam, Tõnu Esko, Tuomas O Kilpeläinen, Zoltán Kutalik, Shengxu Li, Keri L Monda, Anna L Dixon, Christopher C Holmes, Lee M Kaplan, Liming Liang, Josine L Min, Miriam F Moffatt, Cliona Molony, George Nicholson, Eric E Schadt, Krina T Zondervan, Mary F Feitosa, Teresa Ferreira, Hana Lango Allen, Robert J Weyant, Eleanor Wheeler, Andrew R Wood, MAGIC, Karol Estrada, Michael E Goddard, Guillaume Lettre, Massimo Mangino, Dale R Nyholt, Shaun Purcell, Albert Vernon Smith, Peter M Visscher, Jian Yang, Steven A McCarroll, James Nemesh, Benjamin F Voight, Devin Absher, Najaf Amin, Thor Aspelund, Lachlan Coin, Nicole L Glazer, Caroline Hayward, Nancy L Heard-Costa, Jouke-Jan Hottenga, Åsa Johansson, Toby Johnson, Marika Kaakinen, Karen Kapur, Shamika Ketkar, Joshua W Knowles, Peter Kraft, Aldi T Kraja, Claudia Lamina, Michael F Leitzmann, Barbara McKnight, Andrew P Morris, Ken K Ong, John R B Perry, Marjolein J Peters, Ozren Polasek, Inga Prokopenko, Nigel W Rayner, Samuli Ripatti, Fernando Rivadeneira, Neil R Robertson, Serena Sanna, Ulla Sovio, Ida Surakka, Alexander Teumer, Sophie van Wingerden, Veronique Vitart, Jing Hua Zhao, Christine Cavalcanti-Proença, Peter S Chines, Eva Fisher, Jennifer R Kulzer, Cecile Lecoeur, Narisu Narisu, Camilla Sandholt, Laura J Scott, Kaisa Silander, Klaus Stark, Mari-Liis Tammesoo, Tanya M Teslovich, Nicholas John Timpson, Richard M Watanabe, Ryan Welch, Daniel I Chasman, Matthew N Cooper, John-Olov Jansson, Johannes Kettunen, Robert W Lawrence, Niina Pellikka, Markus Perola, Liesbeth Vandenput, Helene Alavere, Peter Almgren, Larry D Atwood, Amanda J Bennett, Reiner Biffar, Lori L

Bonnycastle, Stefan R Bornstein, Thomas A Buchanan, Harry Campbell, Ian N M Day, Mariano Dei, Marcus Dörr, Paul Elliott, Michael R Erdos, Johan G Eriksson, Nelson B Freimer, Mao Fu, Stefan Gaget, Eco J C Geus, Anette P Gjesing, Harald Grallert, Jürgen Gräßler, Christopher J Groves, Candace Guiducci, Anna-Liisa Hartikainen, Neelam Hassanali, Aki S Havulinna, Karl-Heinz Herzig, Andrew A Hicks, Jennie Hui, Wilmar Igl, Pekka Jousilahti, Antti Jula, Eero Kajantie, Leena Kinnunen, Ivana Kolcic, Seppo Koskinen, Peter Kovacs, Heyo K Kroemer, Vjekoslav Krzelj, Johanna Kuusisto, Kirsti Kvaloy, Jaana Laitinen, Olivier Lantieri, G Mark Lathrop, Marja-Liisa Lokki, Robert N Luben, Barbara Ludwig, Wendy L McArdle, Anne McCarthy, Mario A Morken, Mari Nelis, Matt J Neville, Guillaume Paré, Alex N Parker, John F Peden, Irene Pichler, Kirsi H Pietiläinen, Carl G P Platou, Anneli Pouta, Martin Ridderstråle, Nilesh J Samani, Jouko Saramies, Juha Sinisalo, Jan H Smit, Rona J Strawbridge, Heather M Stringham, Amy J Swift, Maris Teder-Laving, Brian Thomson, Gianluca Usala, Joyce B J van Meurs, Gert-Jan van Ommen, Vincent Vatin, Claudia B Volpato, Henri Wallaschofski, G Bragi Walters, Elisabeth Widen, Sarah H Wild, Gonneke Willemsen, Daniel R Witte, Lina Zgaga, Paavo Zitting, John P Beilby, Alan L James, Mika Kähönen, Terho Lehtimäki, Markku S Nieminen, Claes Ohlsson, Lyle J Palmer, Olli Raitakari, Paul M Ridker, Michael Stumvoll, Anke Tönjes, Jorma Viikari, Beverley Balkau, Yoav Ben-Shlomo, Richard N Bergman, Heiner Boeing, George Davey Smith, Shah Ebrahim, Philippe Froguel, Torben Hansen, Christian Hengstenberg, Kristian Hveem, Bo Isomaa, Torben Jørgensen, Fredrik Karpe, Kay-Tee Khaw, Markku Laakso, Debbie A Lawlor, Michel Marre, Thomas Meitinger, Andres Metspalu, Kristian Midthjell, Oluf Pedersen, Veikko Salomaa, Peter E H Schwarz, Tiinamaija Tuomi, Jaakko Tuomilehto, Timo T Valle, Nicholas J Wareham, Alice M Arnold, Jacques S Beckmann, Sven Bergmann, Eric Boerwinkle, Dorret I Boomsma, Mark J Caulfield, Francis S Collins, Gudny Eiriksdottir, Vilmundur Gudnason, Ulf Gyllensten, Anders Hamsten, Andrew T Hattersley, Albert Hofman, Frank B Hu, Thomas Illig, Carlos Iribarren, Marjo-Riitta Jarvelin, W H Linda Kao, Jaakko Kaprio, Lenore J Launer, Patricia B Munroe, Ben Oostra, Brenda W Penninx, Peter P Pramstaller, Bruce M Psaty, Thomas Quertermous, Aila Rissanen, Igor Rudan, Alan R Shuldiner, Nicole Soranzo, Timothy D Spector, Ann-Christine Syvanen, Manuela Uda, André Uitterlinden, Henry Völzke, Peter Vollenweider, James F Wilson, Jacqueline C Witteman, Alan F Wright, Gonçalo R Abecasis, Michael Boehnke, Ingrid B Borecki, Panos Deloukas, Timothy M Frayling, Leif C Groop, Talin Haritunians, David J Hunter, Robert C Kaplan, Kari E North, Jeffrey R O'Connell, Leena Peltonen, David Schlessinger, David P Strachan, Joel N Hirschhorn, Themistocles L Assimes, H-Erich Wichmann, Unnur Thorsteinsdottir, Cornelia M van Duijn, Kari Stefansson, L Adrienne Cupples, Ruth J F Loos, Inês Barroso, Mark I McCarthy, Caroline S Fox, Karen L Mohlke & Cecilia M Lindgren

Description of 14 loci (Supplemental Figure 1)

TBX15-WARS2 (chromosome 1)

There are 3 SNPs (rs984222, rs10923712, rs984225) commonly shared by the credible sets obtained from EA-only and EA+AA. One additional SNP (rs1106529) is included in the EA-only derived credible set while no additional SNP is included in the EA+AA derived credible set. The length changed from 27,654bp for EA-only to 1,591bp for EA+AA derived credible sets. The LD surrounding the original index SNP is slightly stronger in CEU compared (bottom panel) to that in YRI (top panel) although both CEU and YRI have strong LD. The signal in EA sample is strong; the trans-ethnic analysis has slightly enhanced signal and drops one variant in its trans-ethnic derived 95% credible set compared to EA-derived credible set.

DNM3-PIGC (chromosome 1)

There are 9 SNPs (rs9286854, rs991790, rs2227199, rs9425592, rs1011731, rs714515, rs2213732, rs7534393, rs2001129) commonly shared by the credible sets obtained from EA-only and EA+AA. Two additional SNPs (rs9425291, rs2301453) are included in the EA-only derived credible set while one additional SNP (rs2227198) is included in the EA+AA derived credible set. The length changed from 54,037bp for EA-only to 48,775bp for EA+AA derived credible sets. The LD surrounding the original index SNP is stronger in CEU compared to that in YRI. In addition, there is a cluster of variants showing strong association signals in EA-sample. This cluster of variants retains strong association signals in the trans-ethnic analysis although some random fluctuations leads to slight changes of variants included in the credible set.

LYPLAL1 (chromosome 1)

There are 8 SNPs (rs2820443, rs4846567, rs1415288, rs4846302, rs2820446, rs1337101, rs1415293, rs2820441) commonly shared by the credible sets obtained from EA-only and EA+AA. Fifteen additional SNPs (rs2494196, rs3001032, rs2605101, rs2605095, rs2791550, rs2605108, rs2605109, rs2605092, rs2605098, rs2605096, rs7538503, rs12143910, rs2791551, rs2820436, rs2791552) are included in the EA-only derived credible set while no additional SNP is included in the EA+AA derived credible set. The length changed from 148,141bp for EA-only to 27,409bp for EA+AA derived credible sets. The LD surrounding the original index SNP is stronger in CEU compared to that in YRI. In addition, a few SNPs with high LD with the index SNP in both populations have enhanced association signals and the LD block with the index SNP is much narrower in YRI samples, leading to a narrower credible set in trans-ethnic analysis and dropping 15 variants from EA-derived credible set.

GRB14 (chromosome 2)

There are 4 SNPs (rs10195252, rs13389219, rs6717858, rs10184004) commonly shared by the credible sets obtained from EA-only and EA+AA. No additional SNP is included in the EA-only derived credible set while one additional SNP (rs1128249) is included in the EA+AA derived credible set. The length changed from 31,272bp for EA-only to 32,272bp for EA+AA derived credible sets, respectively. The LD block surrounding the original index SNP is wider in EA samples compared to that in YRI samples; however, the block including variants having high LD ($r^2 > 0.6$) with index SNPs are similar between two populations. Five variants standing out from other variants show strong associations in EA samples with one having a slightly weaker signal. The trans-

ethnic analysis enhances all five variants' association signals to the similar level, leading to the inclusion of all five variants in the trans-ethnic analysis derived credible set.

NISCH-STAB1 (chromosome 3)

There are 7 SNPs (rs6784615, rs6445358, rs7614727, rs1010553, rs9853056, rs1060330, rs7614981) commonly shared by the credible sets obtained from EA-only and EA+AA. Three additional SNPs (rs758801, rs1010554, rs4282054) are included in the EA-only derived credible set while another three additional SNPs (rs1108842, rs13083798, rs7622851) are included in the EA+AA derived credible set. The length changed from 277,969bp for EA-only to 431,135bp for EA+AA derived credible sets. There is weak LD surrounding the original index SNP in EA sample. In addition, the signal for the index SNP is weak in EA sample and the trans-ethnic analysis does not enhance association signals (all $\log_{BF} < 6$). Therefore, the credible set in this case may not be informative.

ADAMTS9 (chromosome 3)

There are 7 SNPs (rs4132228, rs4611812, rs4422297, rs4504165, rs6772129, rs6795735, rs9860730) commonly shared by the credible sets obtained from EA-only and EA+AA. Six additional SNPs (rs9864077, rs17676309, rs9311910, rs6445425, rs17727064, rs7428936) are included in the EA-only derived credible set while no additional SNP is included in the EA+AA derived credible set. The length changed from 30,676bp for EA-only to 8,669bp for EA+AA derived credible sets. Neither CEU nor YRI have strong LD with many variants surrounding the original index SNP; however, the variants in strong LD with the index SNP are within a narrow region in both samples of ancestries (narrower in YRI than in CEU). The association signals are highly enhanced and association signals for those top variants are more distinguishable in trans-ethnic analysis compared to EA sample only analysis. These facts lead to the dropping of 6 variants from EA-derived credible set to form a more compact and narrower trans-ethnic analysis derived credible set.

CPEB4 (chromosome 5)

There are 11 SNPs (rs10516107, rs966544, rs747472, rs7736263, rs17695092, rs1976074, rs7705502, rs1484803, rs17696407, rs6882088, rs6861681) commonly shared by the credible sets obtained from EA-only and EA+AA. No additional SNP is included in the EA-only derived credible set while one additional SNP (rs1564823) is included in the EA+AA derived credible set. The length changed from 93,159bp for EA-only to 93,159bp for EA+AA derived credible sets. The association signals within this locus are weak in the EA-sample and EA+AA sample ($\log_{BF} < 6$). Therefore, their relevant credible sets are not informative.

LY86 (chromosome 6)

There are 4 SNPs (rs1294410, rs1294421, rs1294407, rs912056) commonly shared by the credible sets obtained from EA-only and EA+AA. Two additional SNPs (rs1294438, rs912057) are included in the EA-only derived credible set while one additional SNP (rs1294409) is included in the EA+AA derived credible set. The length changed from 15,862bp for EA-only to 6,952bp for EA+AA derived credible sets. The LD block surrounding the index SNP is narrow in both samples of ancestries, but it is narrower in

YRI. The association signals are enhanced for some variants in trans-ethnic analysis and these significant variants form a cluster clearly separated from other variants in regional association plot. The weaker LD and stronger association signals lead to a narrower credible set in trans-ethnic analysis.

VEGFA (chromosome 6)

There is 1 SNP (rs1358980) commonly shared by the credible sets obtained from EA-only and EA+AA. One additional SNP (rs6905288) is included in the EA-only derived credible set while one additional SNP (rs2998584) is included in the EA+AA derived credible set. The length changed from 6,678bp for EA-only to 6,655bp for EA+AA derived credible sets. There is very weak LD with the index SNP in both samples of ancestries. There is clearly a cluster of three variants significantly associated with phenotype WHR-BMI in both EA-only and trans-ethnic analysis; however, the signals were stronger in trans-ethnic analysis. Some random fluctuations lead to the slight change in the rank of association signals for these three variants and hence the variants included in credible sets.

RSPO3 (chromosome 6)

There are 18 SNPs (rs7766106, rs9491696, rs4382293, rs1936809, rs1936807, rs1892172, rs4424101, rs13204656, rs7742668, rs6916318, rs7775715, rs2326565, rs9285458, rs1936801, rs9491704, rs9491701,, rs3734626) commonly shared by the credible sets obtained from EA-only and EA+AA. Fifteen additional SNP (rs2745353, rs1936805, rs2503322, rs4566896, rs4644087, rs2503107, rs2489623, rs2800708, rs6569474, rs11154386, rs1936802, rs2503109, rs2503326, rs9491703, rs2326566) are included in the EA-only derived credible set while two additional SNPs (rs1936806, rs9482770) are included in the EA+AA derived credible set. The length changed from 66,820bp for EA-only to 60,186bp for EA+AA derived credible sets. The LD surrounding the index SNP is quite similar between CEU and YRI but the index SNP is in LD with fewer variants in YRI. Many variants in LD with the index SNP show strong association signals in EA sample and in the trans-ethnic analysis the association signals are enhanced. Due to the similar pattern of LD and association signal, we do not observe dramatic change in the credible sets but only observe slightly narrower credible set in trans-ethnic analysis.

NFE2L3 (chromosome 7)

There are 10 SNPs (rs4141278, rs10245353, rs1055144, rs2893221, rs10267498, rs10282436, rs9987000, rs2391168, rs11770186, rs10260677) commonly shared by the credible sets obtained from EA-only and EA+AA. Three additional SNP (rs10238703, rs10951112, rs12666961) are included in the EA-only derived credible set while no additional SNP is included in the EA+AA derived credible set. The length changed from 38,160bp for EA-only to 36,707bp for EA+AA derived credible sets. The LD surrounding the index SNP is stronger in CEU compared to that in YRI but the variants in high LD ($r^2 > 0.6$) span a similar range. A clear cluster of variants in LD with the index SNP shows strong association signals in both EA sample analysis and trans-ethnic analysis. Due to the similar pattern of LD and strength of association signals, we do not observe dramatic change in the credible sets but only observe slightly narrower credible set in trans-ethnic analysis.

ITPR2-SSPN (chromosome 12)

There are 7 SNPs (rs7302344, rs1049380, rs1049376, rs11048456, rs10842708, rs7132434, rs1463679) commonly shared by the credible sets obtained from EA-only and EA+AA. Six additional SNPs (rs718314, rs1872992, rs10842703, rs1027087, rs2137564, rs10842707) are included in the EA-only derived credible set while one additional SNP (rs11048470) is included in the EA+AA derived credible set. The length changed from 38,192bp for EA-only to 28,393bp for EA+AA derived credible sets. The LD surrounding the index SNP is weaker in YRI compared to CEU and the association signals are strongly enhanced in trans-ethnic analysis. These facts lead to the dropping several variants to form a narrower trans-ethnic analysis derived credible set.

HOXC13 (chromosome 12)

There are 3 SNPs (rs1443512, rs1822438, rs10783615) commonly shared by the credible sets obtained from EA-only and EA+AA. No additional SNP is included in the EA-only derived credible set and no additional SNP is included in the EA+AA derived credible set. The length changed from 7,447bp for EA-only to 7,447bp for EA+AA derived credible sets. There is stronger LD in this locus in CEU compared to in the YRI but three variants, clearly separately from other variants, show strong association signals in both EA sample analysis and trans-ethnic analysis. These three variants comprise the 95% credible sets for both analyses.

ZNRF3-KREMEN1 (chromosome 22)

There are 2 SNPs (rs4823006, rs2294239) commonly shared by the credible sets obtained from EA-only and EA+AA. One additional SNP (rs2179129) is included in the EA-only derived credible set while no additional SNP is included in the EA+AA derived credible set. The length changed from 2,194bp for EA-only to 2,194bp for EA+AA derived credible sets. There were very few variants having strong LD ($r^2 > 0.6$) with index SNP and these variants span a quite narrow region in both YRI and CEU. Therefore, we observe no dramatic changes in their relevant credible sets.

Supplementary Table 1. Analysis method of ENCODE and Roadmap Epigenomics datasets used to annotate regulatory evidence. Method of analysis for ENCODE (integrative analysis or standard analysis) and Roadmap Epigenomics data (IDR or MAC2 alone) used in epigenomics analysis. Numbers in parentheses indicate the number of datasets when more than one is available. IDR=Irreproducible Discovery Rate, TF=Transcription Factor Binding.

ENCODE Consortium									
Sample	Tissue	DNase	H3K4me1	H3K27ac	H3K4me3	H3K9ac	FAIRE	H3K4me2	TF
GM12878	Blood	Integrative	Integrative	Integrative	Integrative (2)	Integrative	Integrative	Integrative	Integrative (75)
Astrocytes	Brain	Integrative	Standard	Integrative	Integrative	-	Integrative	-	Integrative (1)
Cerebellum	Brain	Standard	-	-	-	-	-	-	-
Cerebral Frontal	Brain	Standard	-	-	-	-	-	-	-
Frontal Cortex	Brain	Standard	-	-	-	-	Integrative	-	-
HUVEC	Endothelial	Integrative	Integrative	Integrative	Integrative (2)	Integrative	Integrative	Integrative	Integrative (11)
HepG2	Liver	Integrative	Integrative	Integrative	Integrative (2)	Integrative	Integrative	Integrative	Integrative (61)
Hepatocytes	Liver	Integrative	-	-	-	-	-	-	-
Huh-7	Liver	Integrative	-	-	-	-	-	-	-
Myocyte	Muscle	Integrative	Integrative	Integrative	Integrative	Integrative	-	Integrative	Integrative (1)
Myotube	Muscle	Integrative	Integrative	Integrative	Integrative	Integrative	-	Integrative	Integrative (1)
Psoas Muscle	Muscle	Standard	-	-	-	-	-	-	-
Differentiated Pancreatic Islets	Pancreatic Islet	Standard	-	-	-	-	-	-	-
Pancreatic Islet	Pancreatic Islet	Integrative	-	-	-	-	Integrative	-	-
Roadmap Epigenomics Project									
Sample	Tissue	DNase	H3K4me1	H3K27ac	H3K4me3	H3K9ac	FAIRE	H3K4me2	TF
Adipose Nuclei	Adipose	-	IDR	MACS2	IDR	IDR	-	-	-
Anterior Caudate	Brain	-	IDR	MACS2	IDR	MACS2	-	-	-
Mid Frontal Lobe	Brain	-	IDR	MACS2	IDR	MACS2	-	-	-
Substantia Nigra	Brain	-	IDR	-	IDR	MACS2	-	-	-
Adult Liver	Liver	-	IDR	-	IDR	IDR	-	-	-
Skeletal Muscle	Muscle	-	IDR	MACS2	IDR	IDR	-	-	-
Pancreatic Islet	Pancreatic Islet	-	MACS2	-	MACS2	MACS2	-	-	-

Supplementary Table 2. SNPs in LD with Credible Set SNPs that Overlap Regulatory Data. For loci with >25% decrease in credible region size, SNPs in LD with credible set SNPs are shown if they overlap two or more regulatory datasets in the same tissue. Negative distance from nearest GENCODE v12 basic annotation TSS indicates the variant is downstream of the TSS relative to the direction of transcription. Tissues with elements overlapping each SNP are indicated as A=Adipose, B=Blood, E=Endothelial, I=Pancreatic Islets, L=Liver, M=Muscle, N=Brain, O=Bone; Chr=Chromosome, TSS=Transcription Start Site

SNPs in LD with Credible set SNPs ($r^2 > .8$)					Linkage Disequilibrium				Regulatory Datasets Overlapping SNPs (by Tissue)						
SNP	Chr	Position	Nearest Coding TSS	EUR CR	EUR	AFR CR	AFR	Na	Open Chromatin ^b	H3K4me1	H3K27ac	H3K4me3	H3K9ac	H3K4me2	
					LD (r ²)		LD (r ²)								
TBX15-WARS2															
rs1409157	1	119,504,487	25,941	TBX15	rs984225	1.00	rs984225	0.99	15	B	AOML	AOML	L	L	OL
rs10923713	1	119,510,487	19,941	TBX15	rs10923712	1.00	rs10923712	0.98	4		AML	A			
rs10802069	1	119,517,357	13,071	TBX15	rs10923712	0.99	rs10923712	0.86	9	M	M	AOM			M
ADAMTS9															
rs4368494c	3	64,701,387	-27,711	ADAMTS9	rs4504165	0.99	rs4132228	0.74	4			AM		M	
rs62247658	3	64,715,155	-41,479	ADAMTS9	rs4611812	0.98	rs6795735	0.95	3		M	M		M	
LY86															
rs1294406c	6	6,737,737	148,810	LY86	rs1294409	0.99	rs1294421	0.30	18	M	AOM	AM	AOMNIE		OME
rs1294418	6	6,742,185	153,258	LY86	rs1294421	0.99	rs1294421	0.97	5	M	L	M			
rs1294430	6	6,744,698	155,771	LY86	rs1294421	1.00	rs1294421	1.00	3	LB	L				
rs1294436c	6	6,746,166	157,239	LY86	rs1294421	0.97	rs1294409	0.41	6		ML	M	M	M	
rs1294437c	6	6,749,789	160,862	LY86	rs912056	0.85	rs1294421	0.52	19		AOMNL	AM	AOML	M	ML

^aNumber indicates the total number of overlapping data sets across experiments and cell types

^bOverlap with FAIRE and/or DNaseI hypersensitivity elements indicates open chromatin

^cSNP exceeded the LD threshold of $r^2 > 0.8$ in EUR only

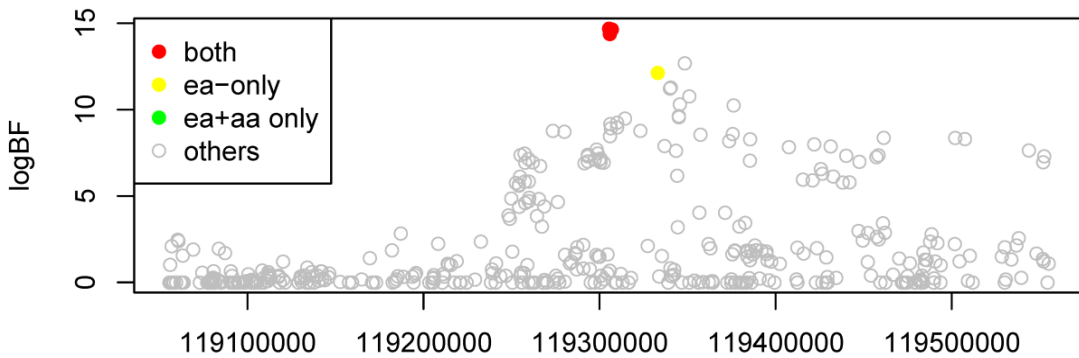
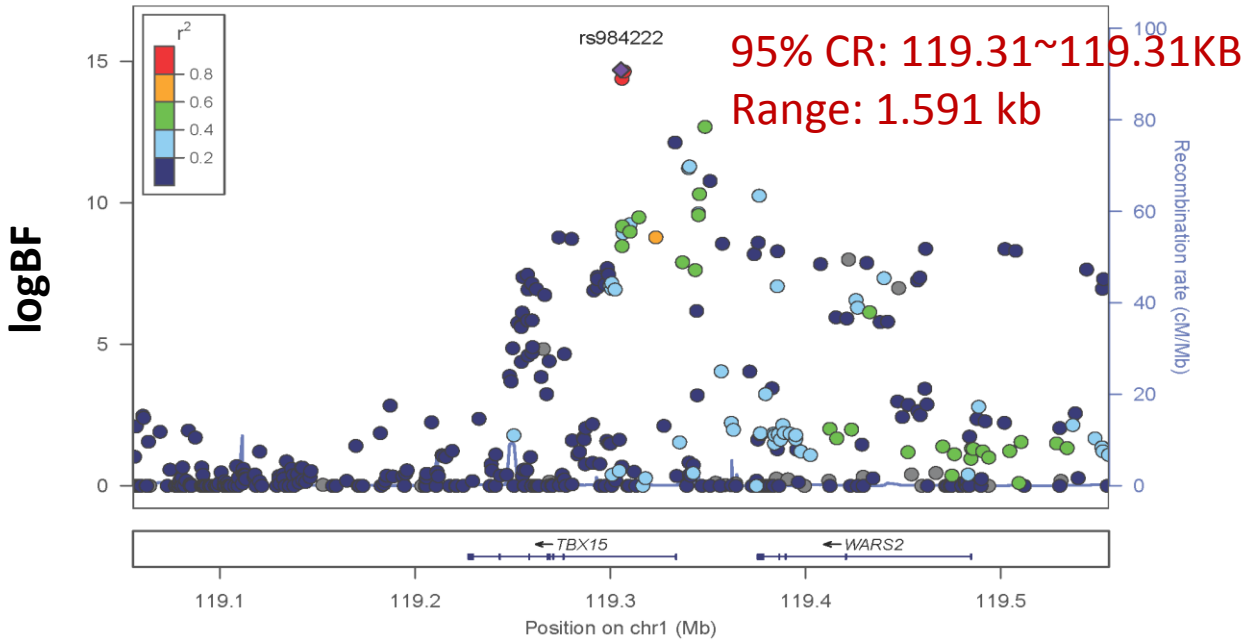
Supplementary Figure 1. Regional Plot of 14 Loci. The top panel on each plot is the trans-ethnic meta-analysis result of EA+AA sample with HapMap II YRI linkage disequilibrium information.

The middle panel displays the classification of each variant to whether it is included in the credible set. The bottom panel is from EA sample only analysis with HapMAP II CEU linkage disequilibrium information.

TBX15-WARS2

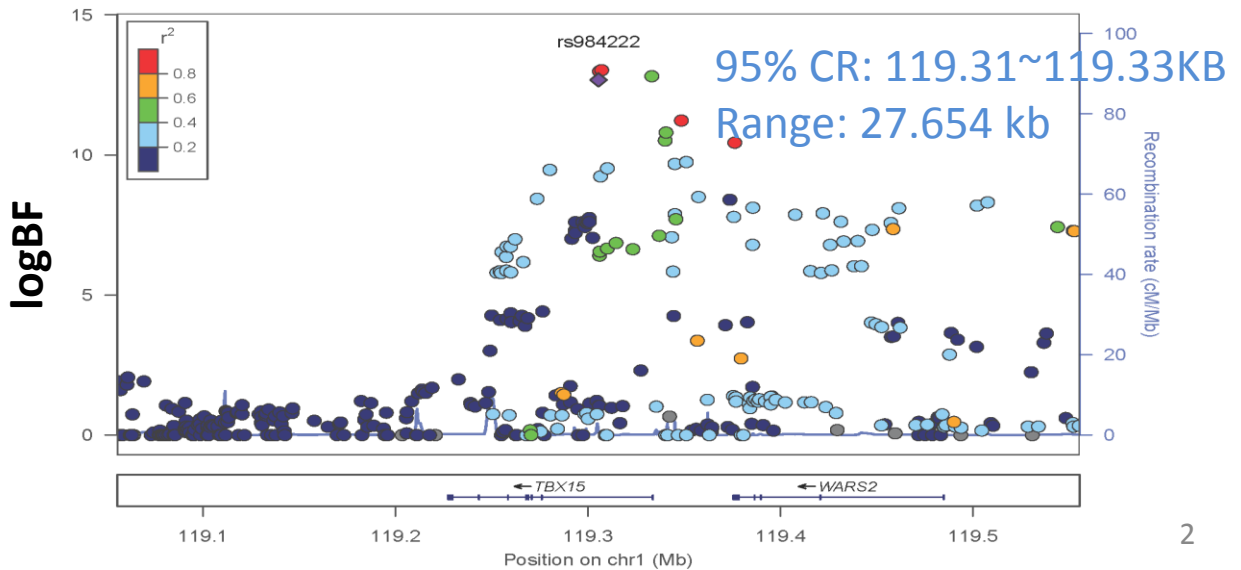
rs984222

Plotted SNPs



EA Sample Only Result: rs984222

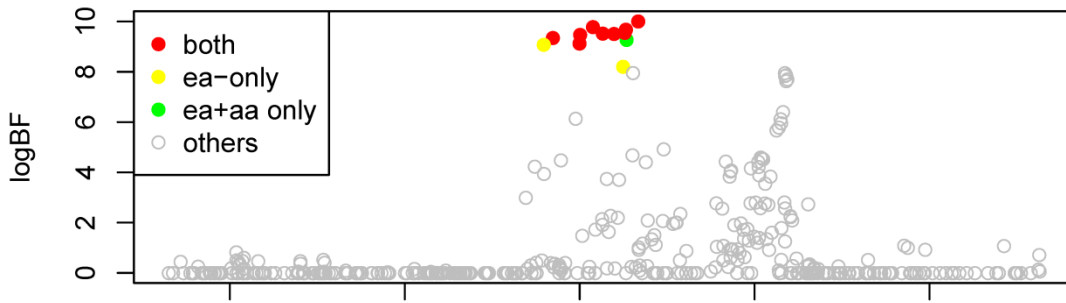
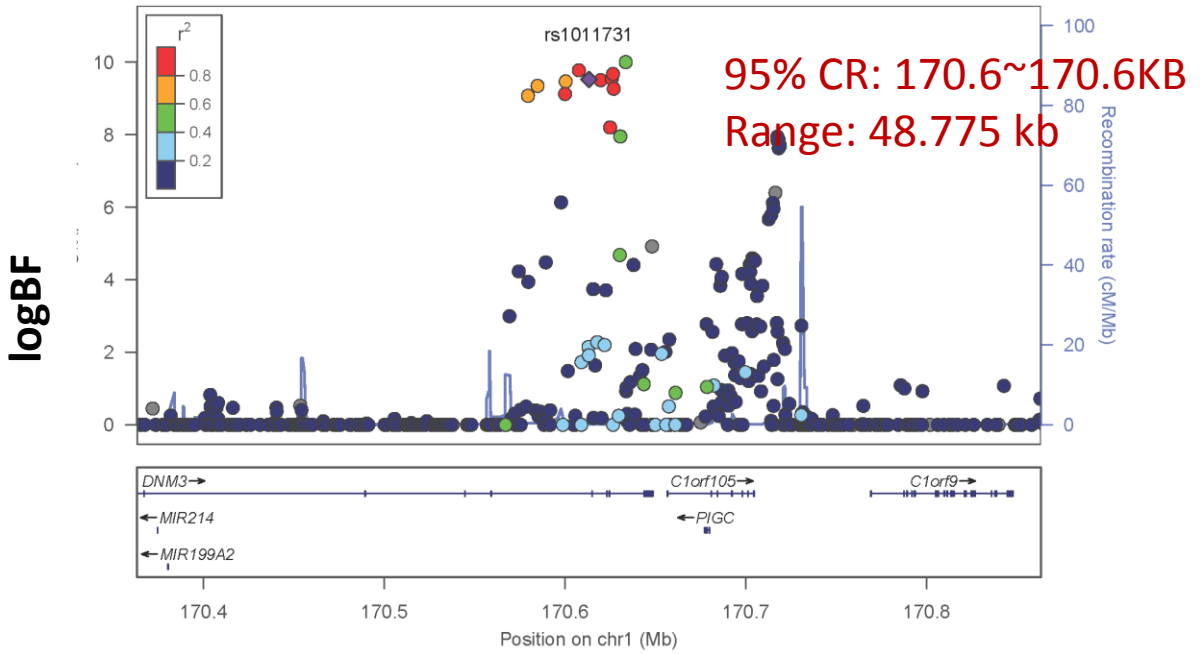
Plotted SNPs



DNM3-PIGC

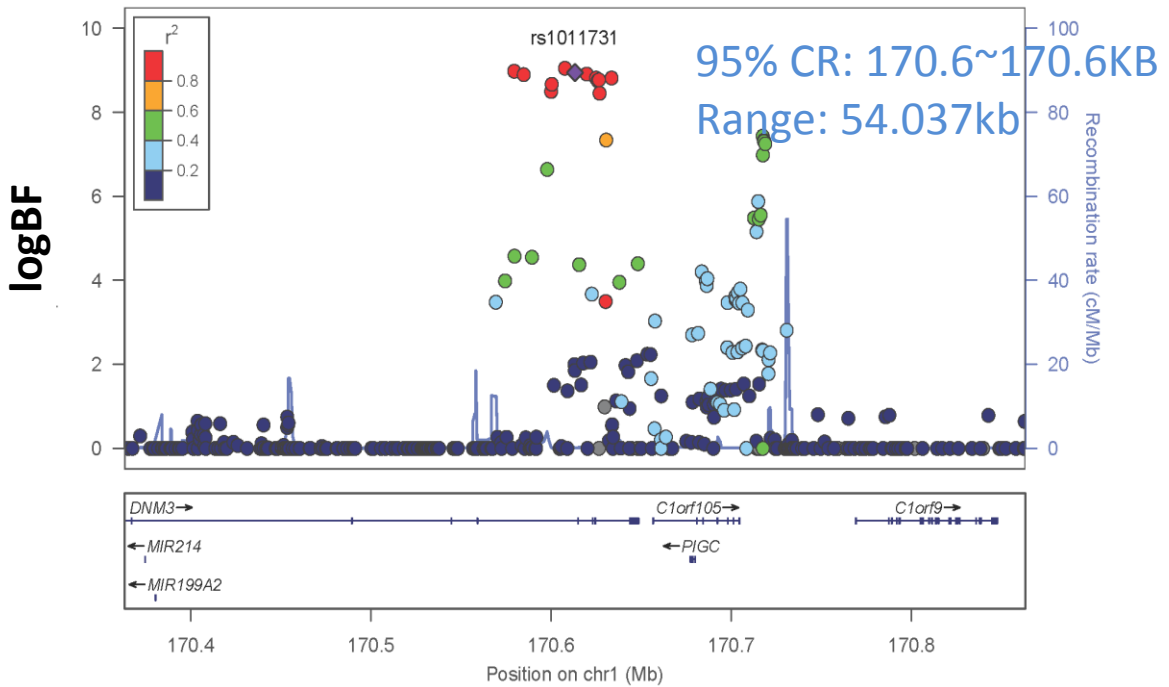
rs1011731

Plotted SNPs

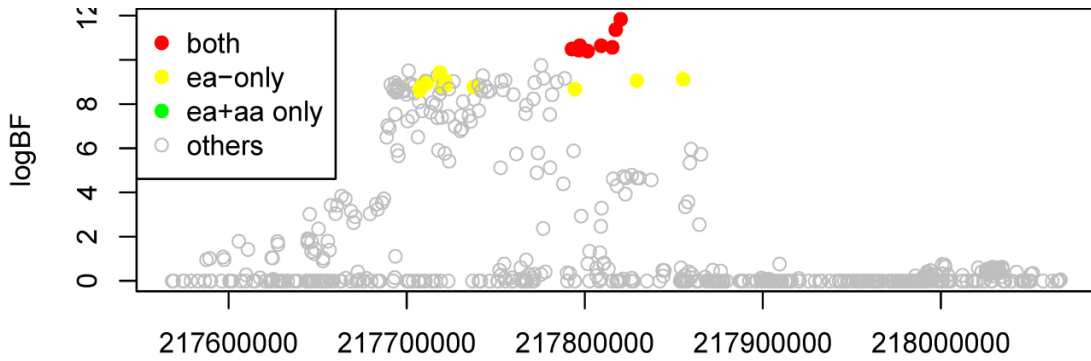
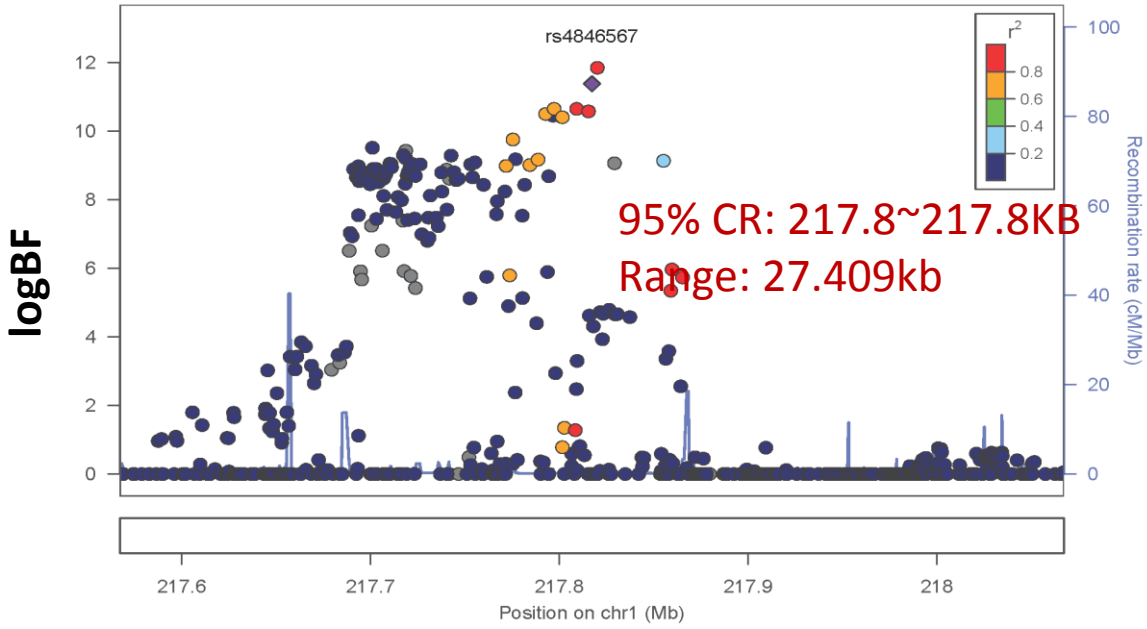


EA Sample Only Result: rs1011731

Plotted SNPs

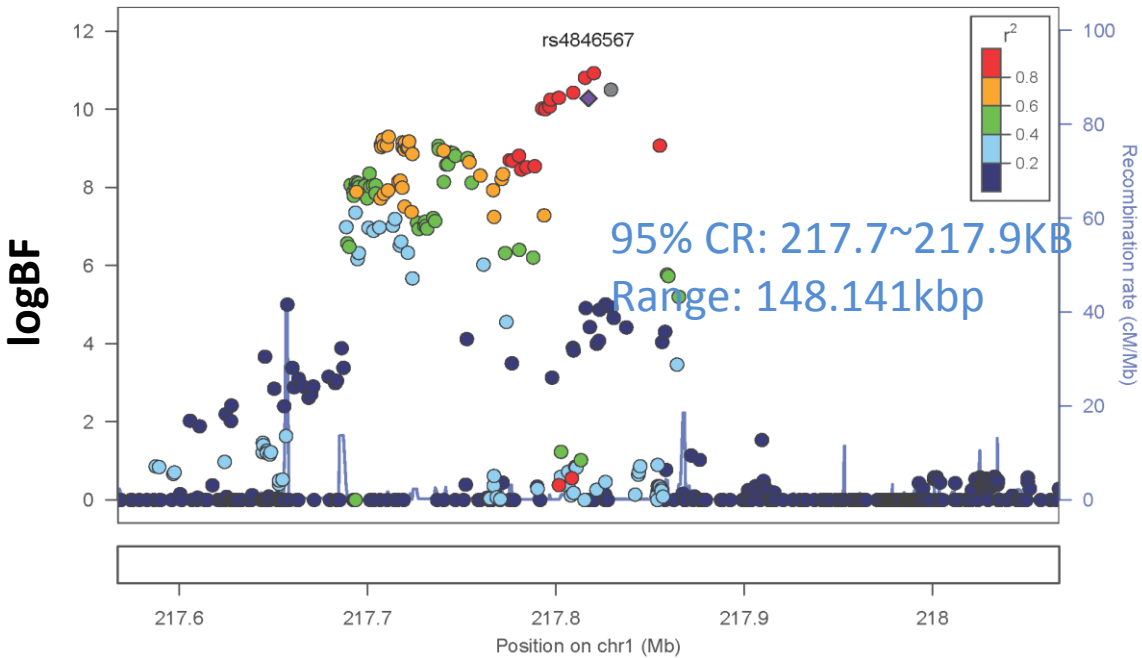


Plotted SNPs

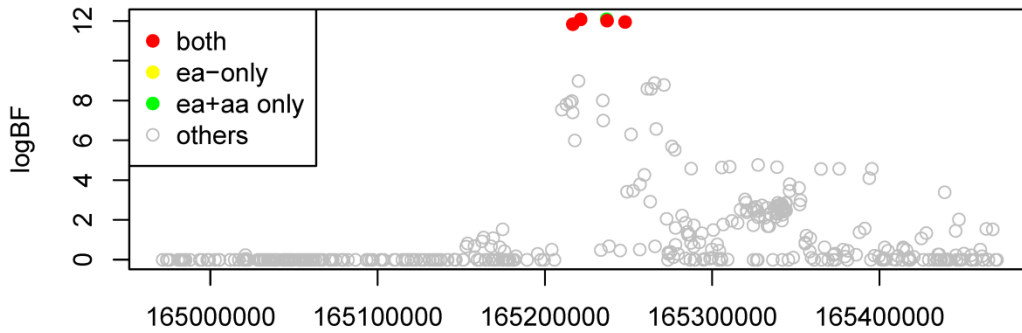
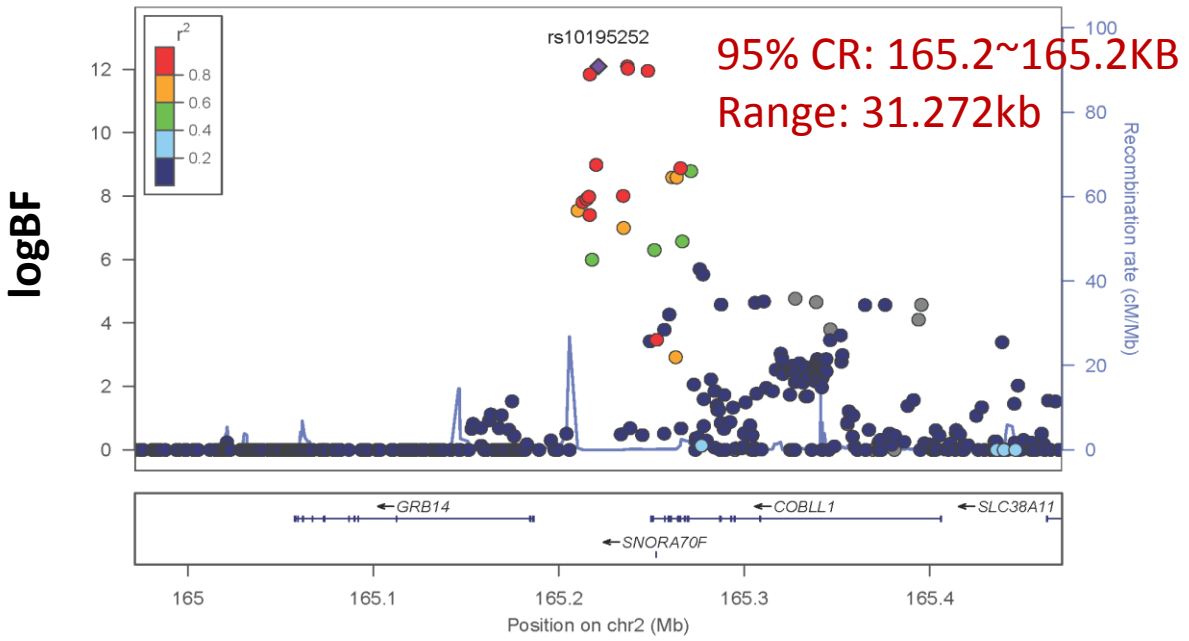


EA Sample Only Result: rs4846567

Plotted SNPs

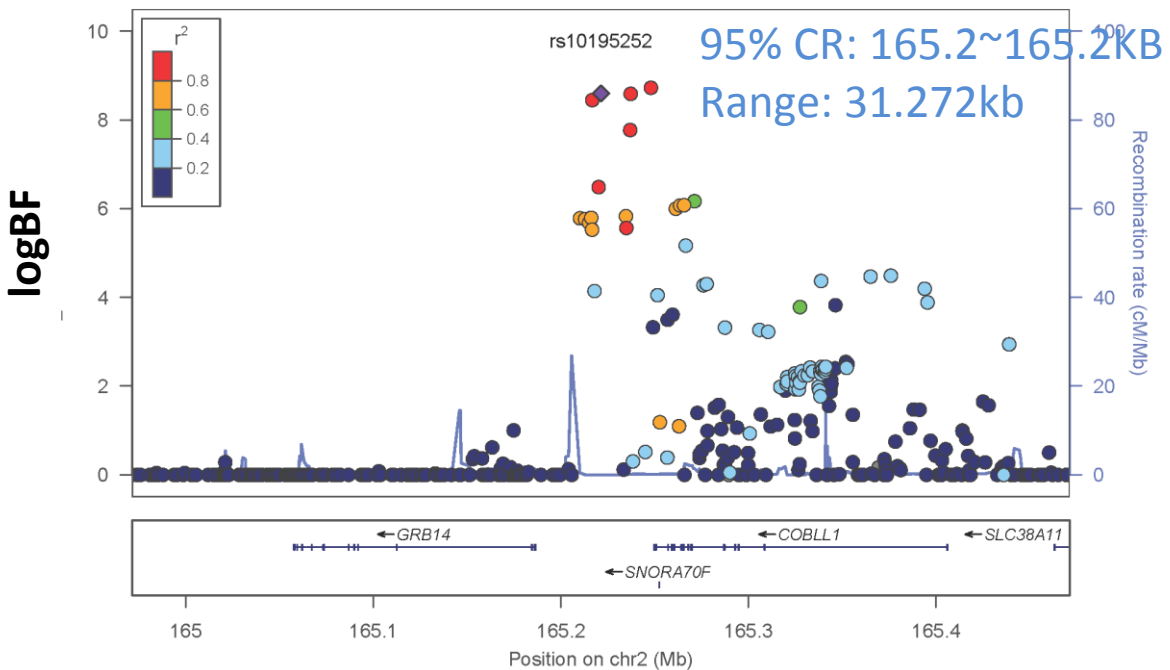


Plotted SNPs



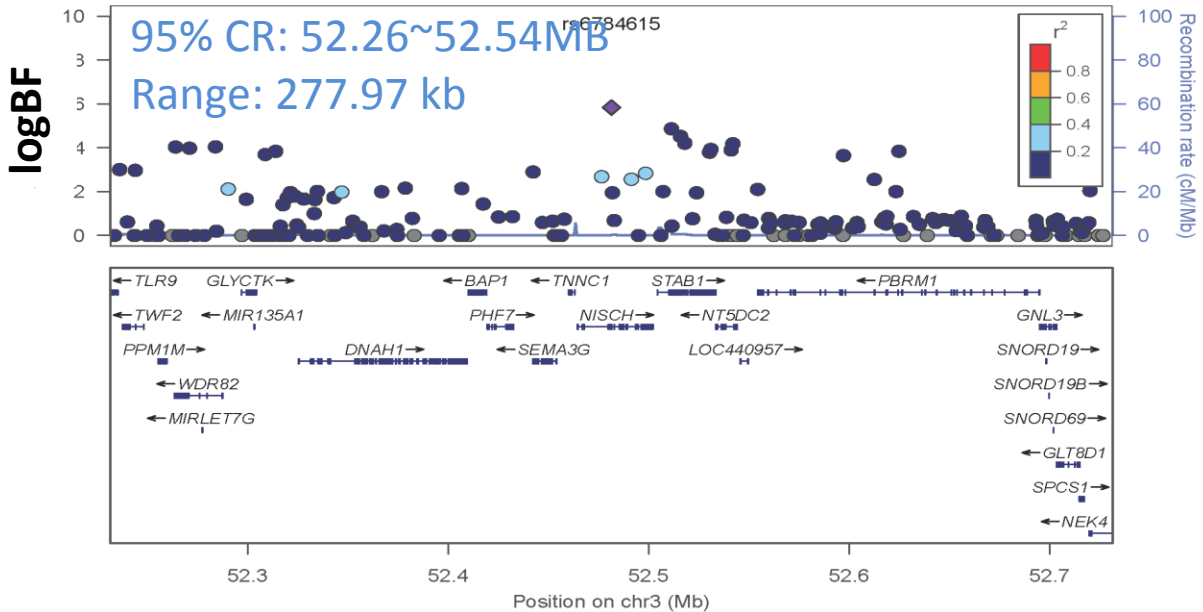
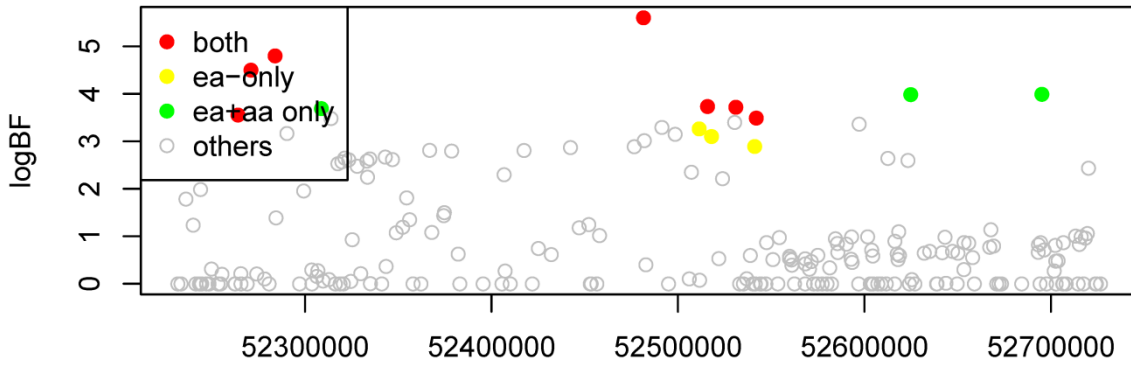
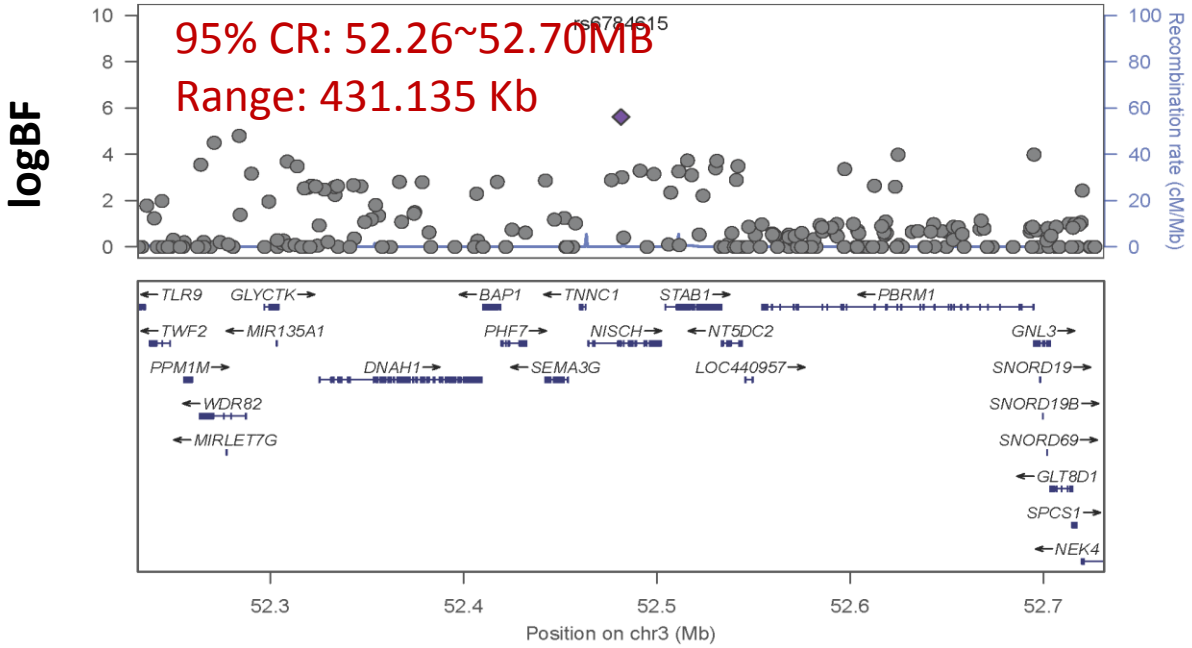
EA Sample Only Result: rs10195252

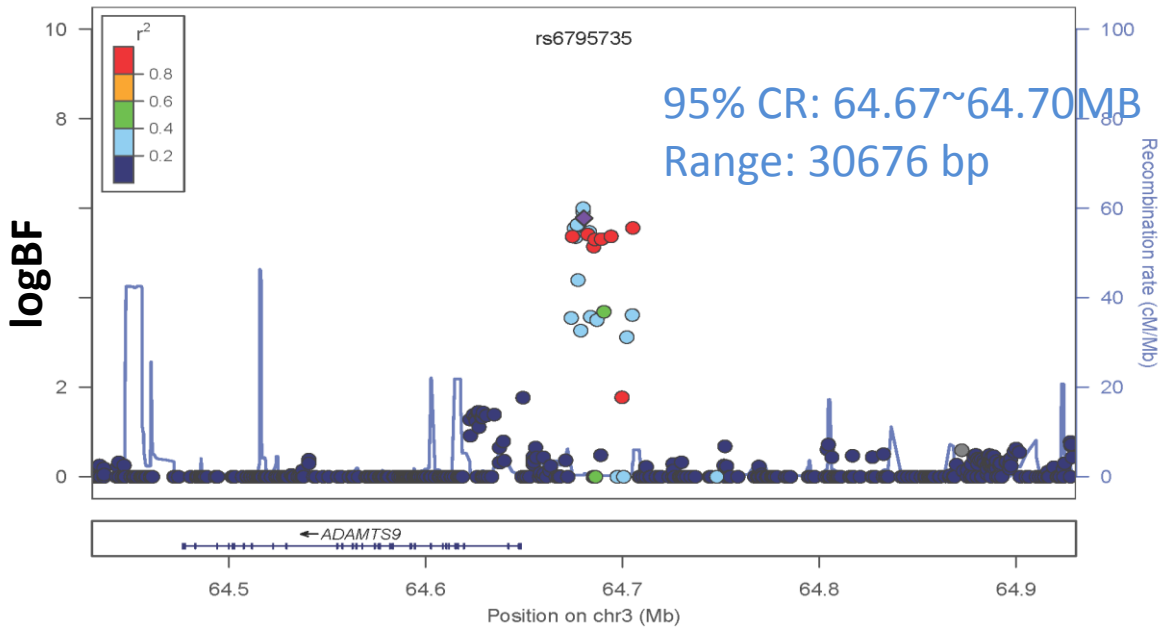
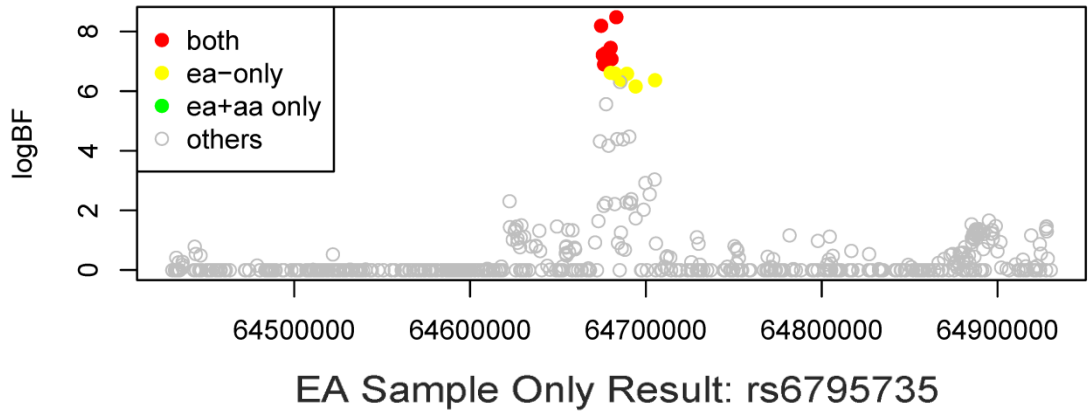
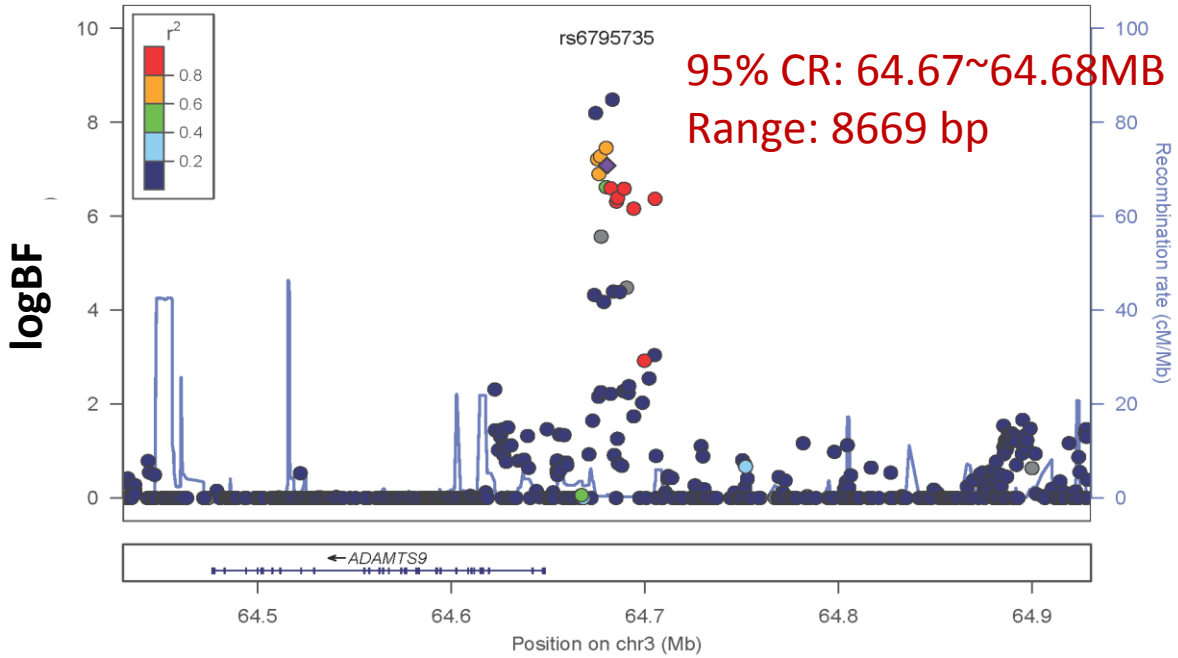
Plotted SNPs



NISCH-STAB1

rs6784615

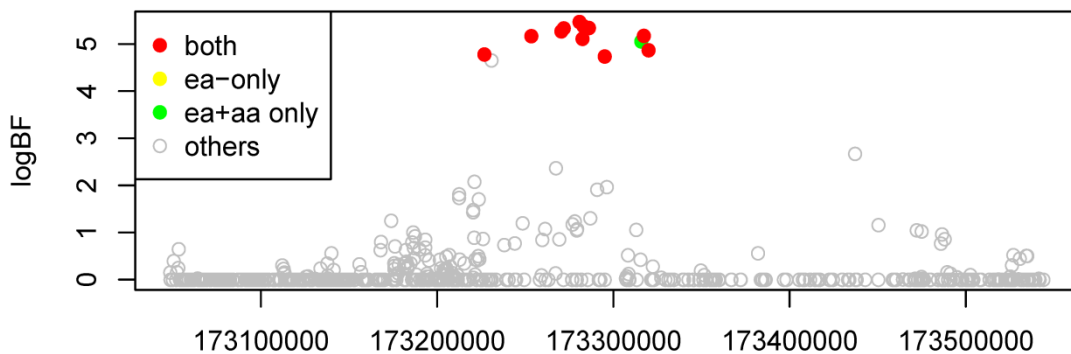
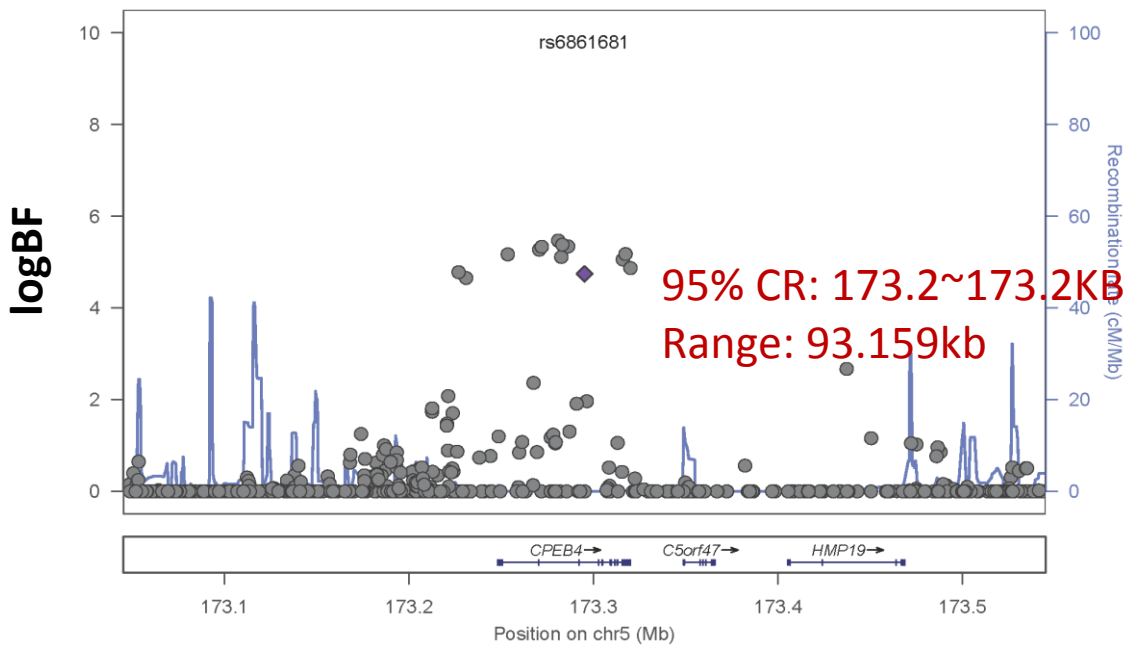




rs6861681

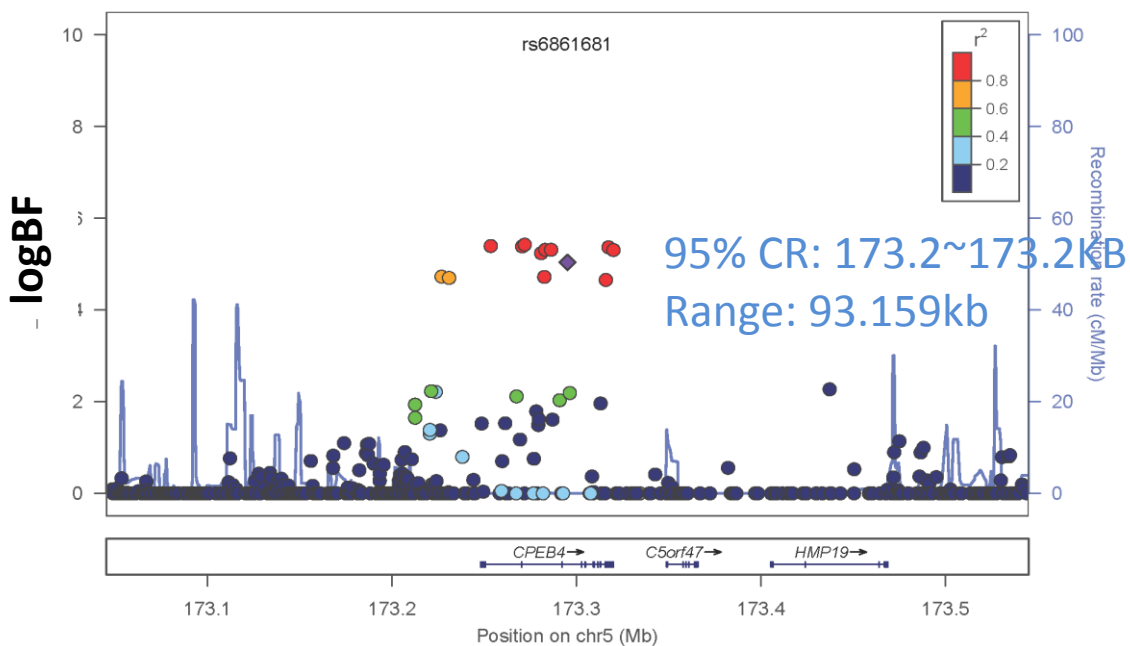
CPEB4

Plotted SNPs



EA Sample Only Result: rs6861681

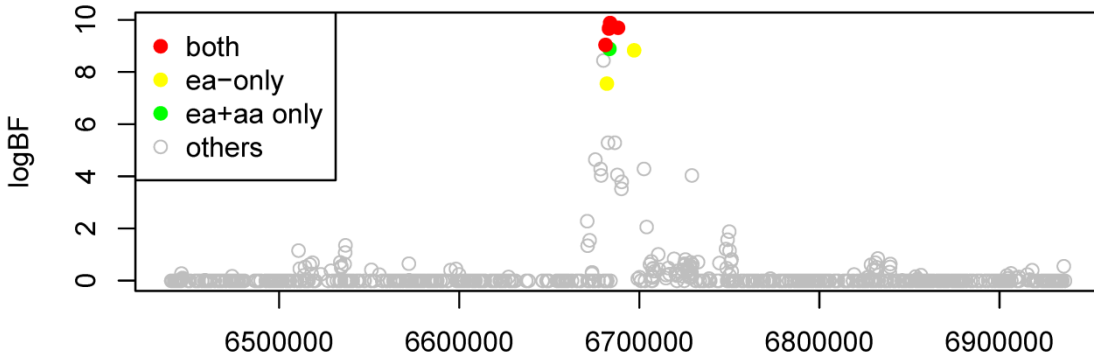
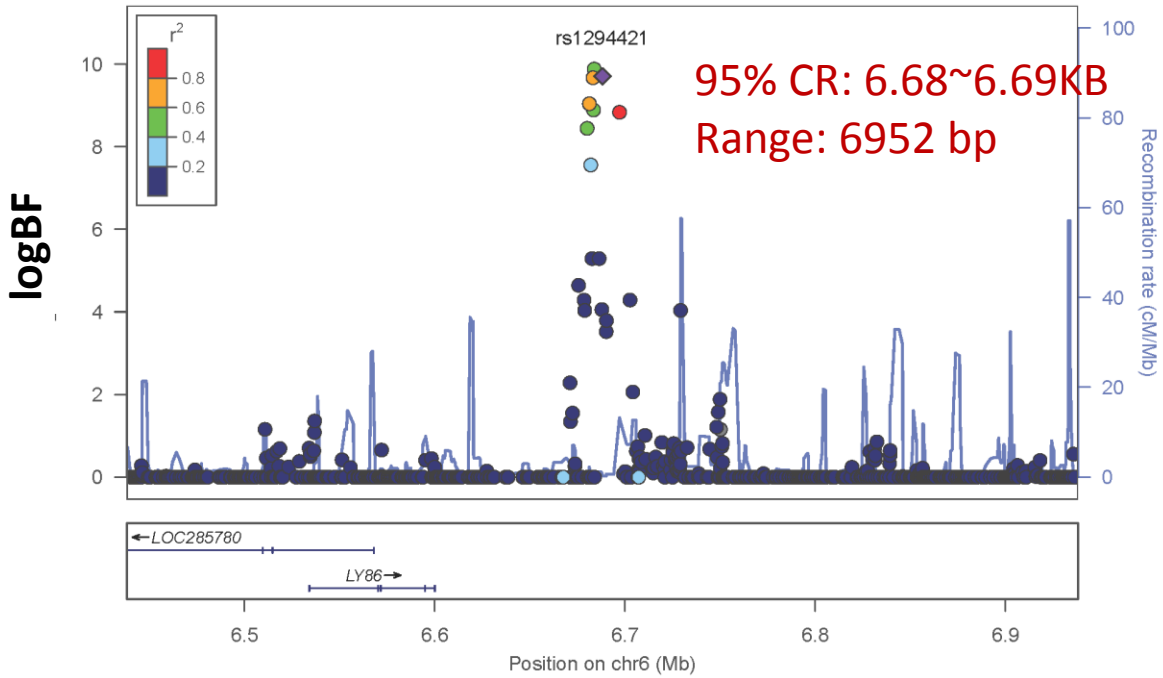
Plotted SNPs



LY86

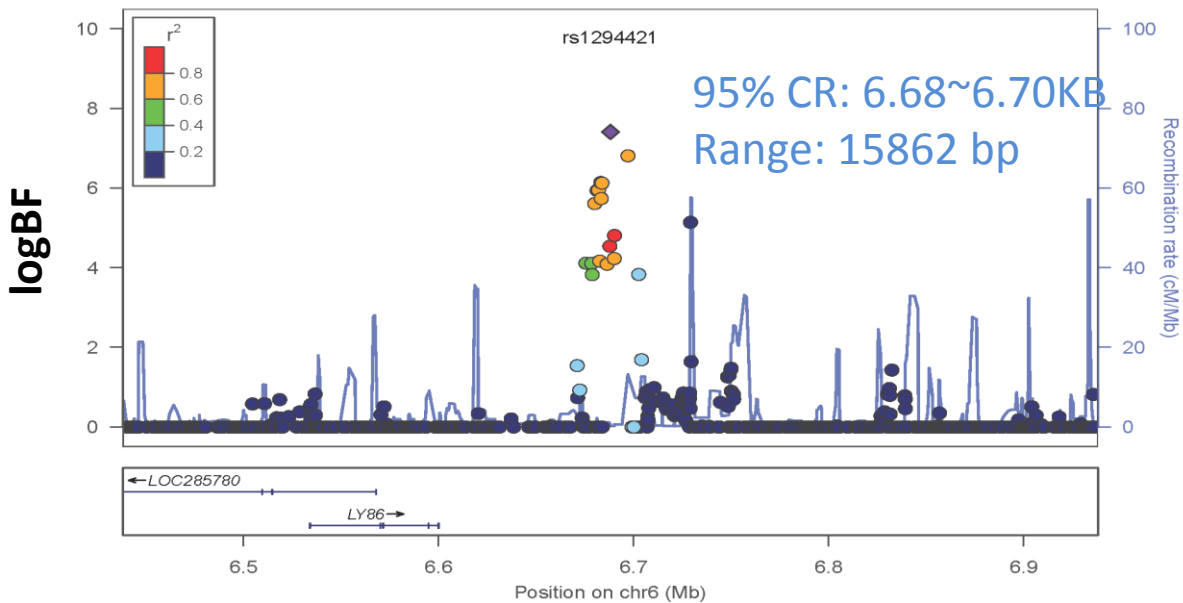
rs1294421

Plotted SNPs



EA Sample Only Result: rs1294421

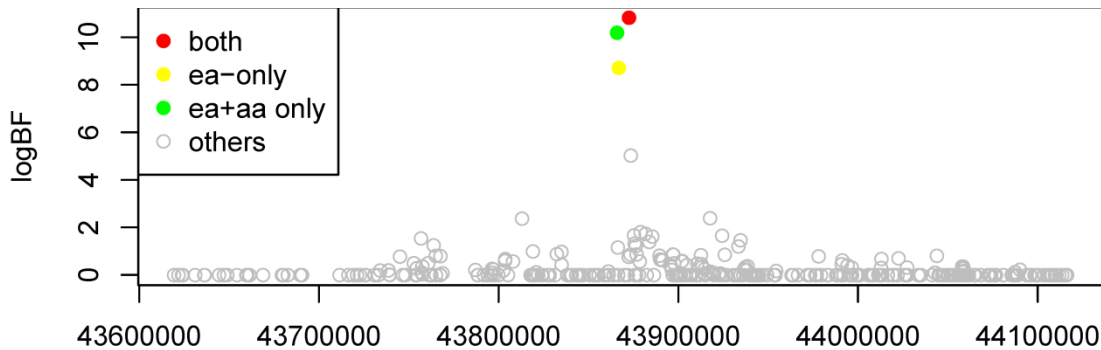
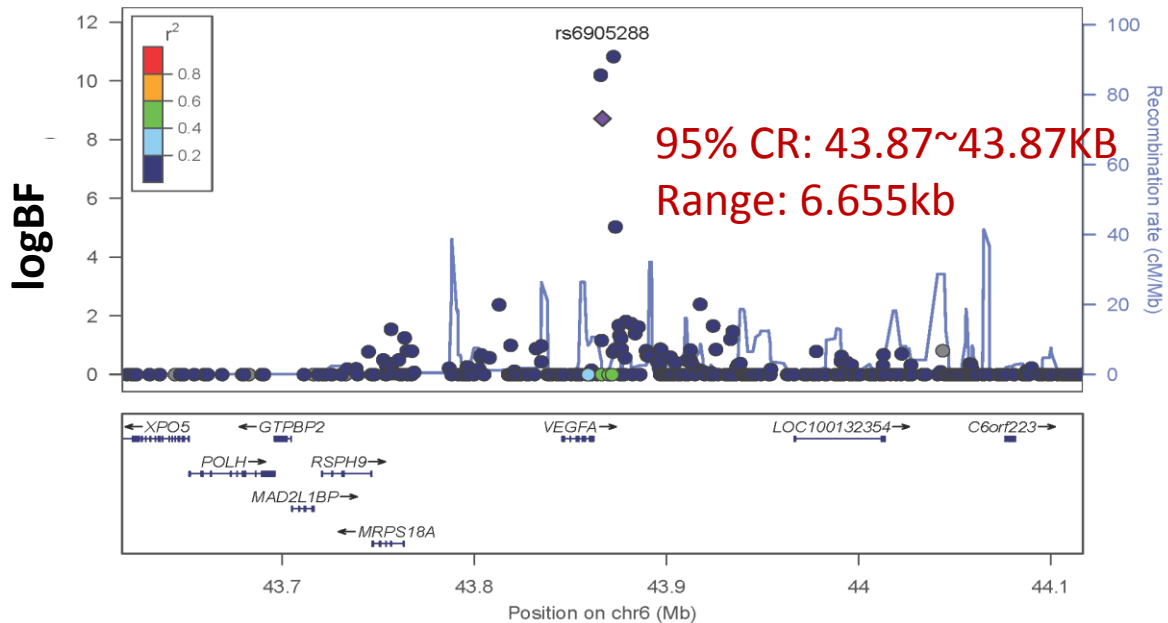
Plotted SNPs



VEGFA

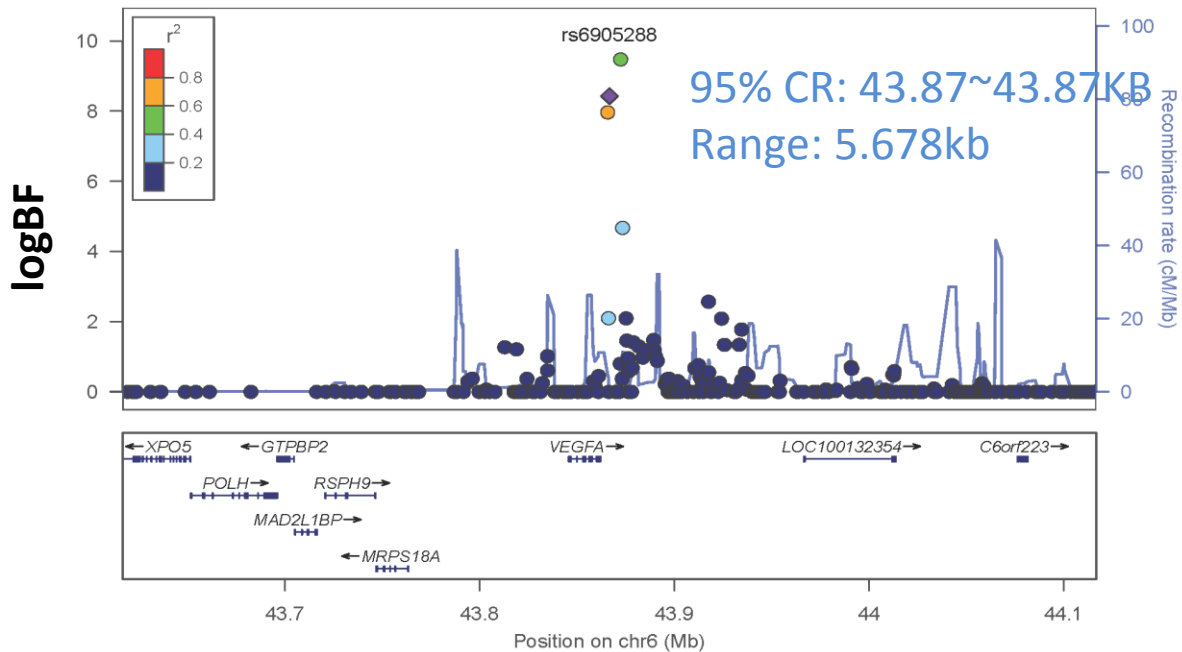
rs6905288

Plotted SNPs



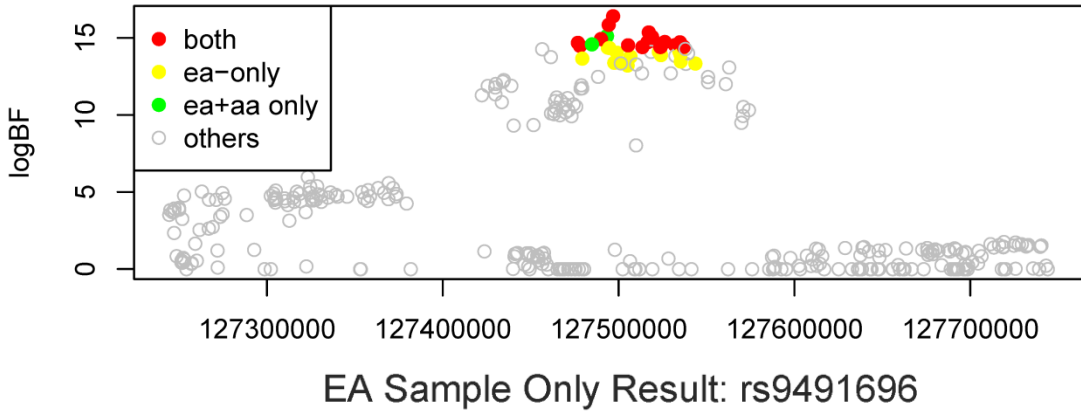
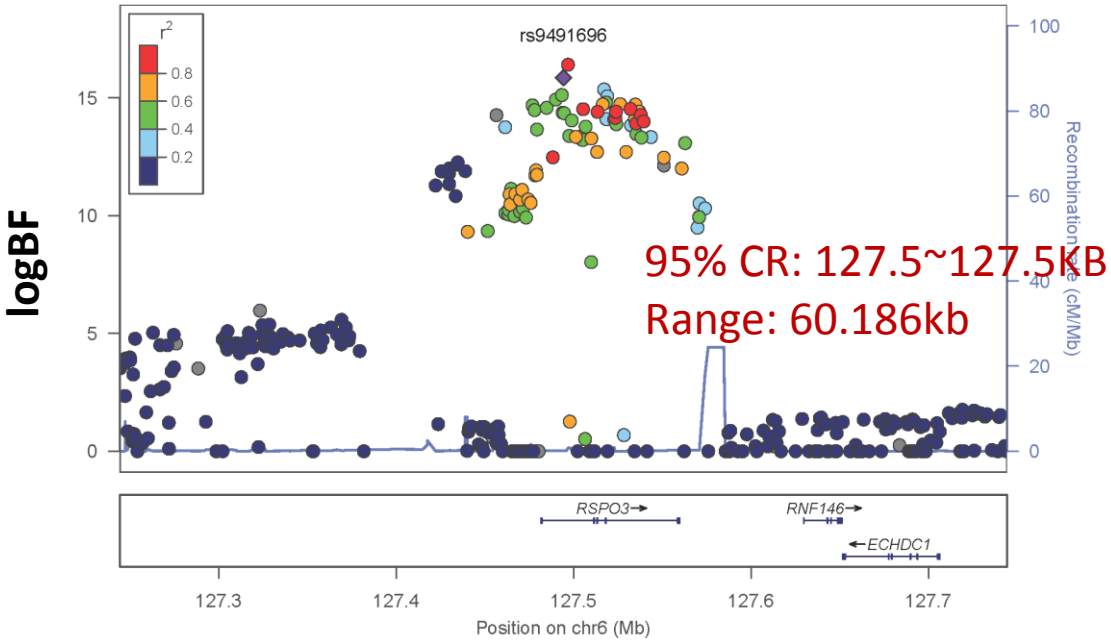
EA Sample Only Result: rs6905288

Plotted SNPs



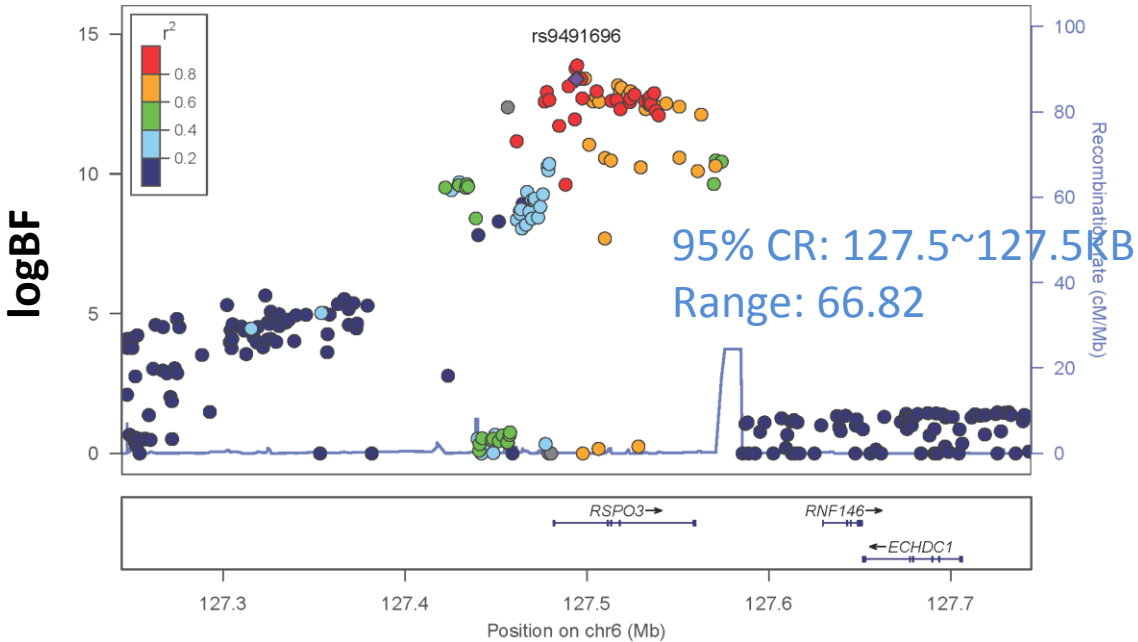
Plotted SNPs

Plotted SNPs

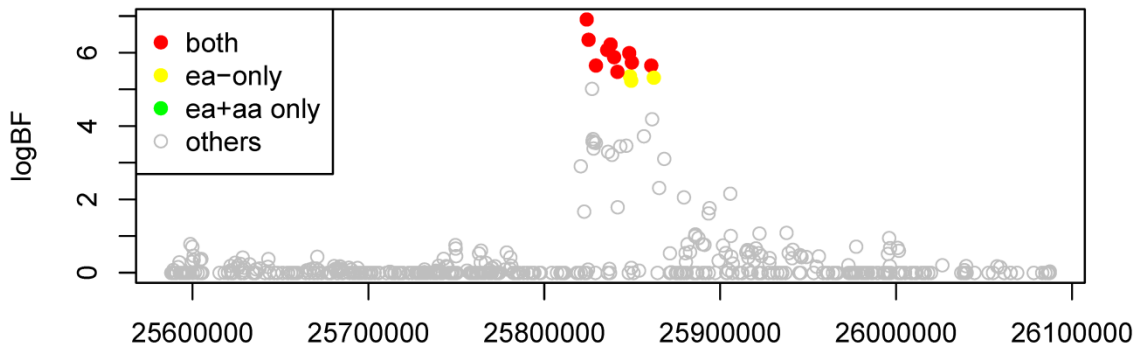
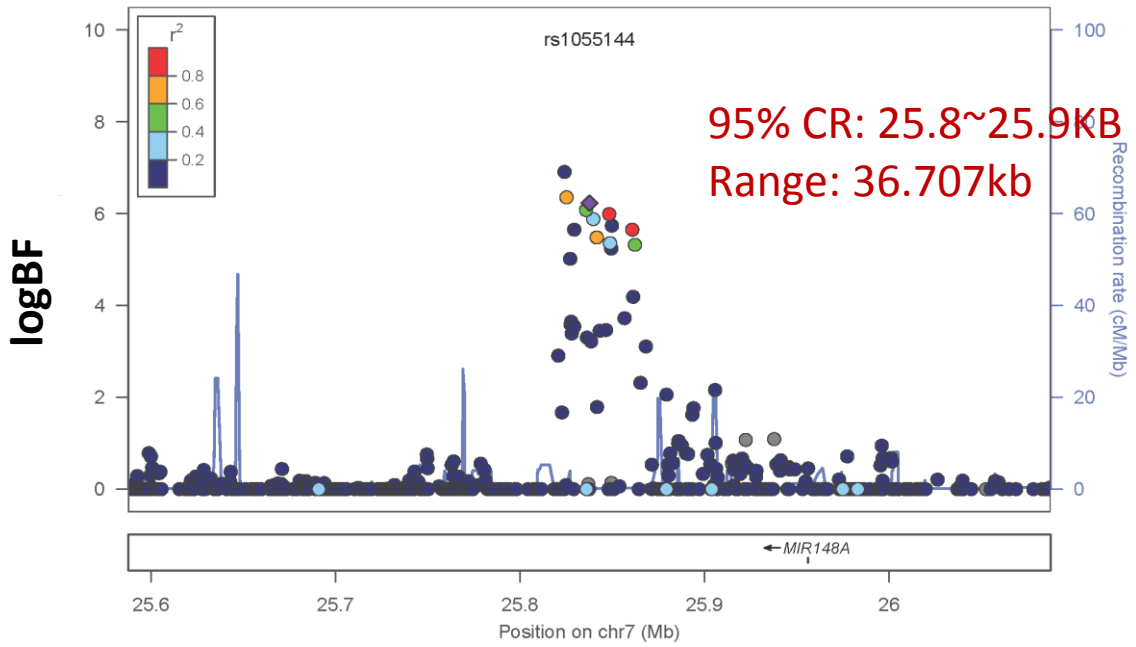


Plotted SNPs

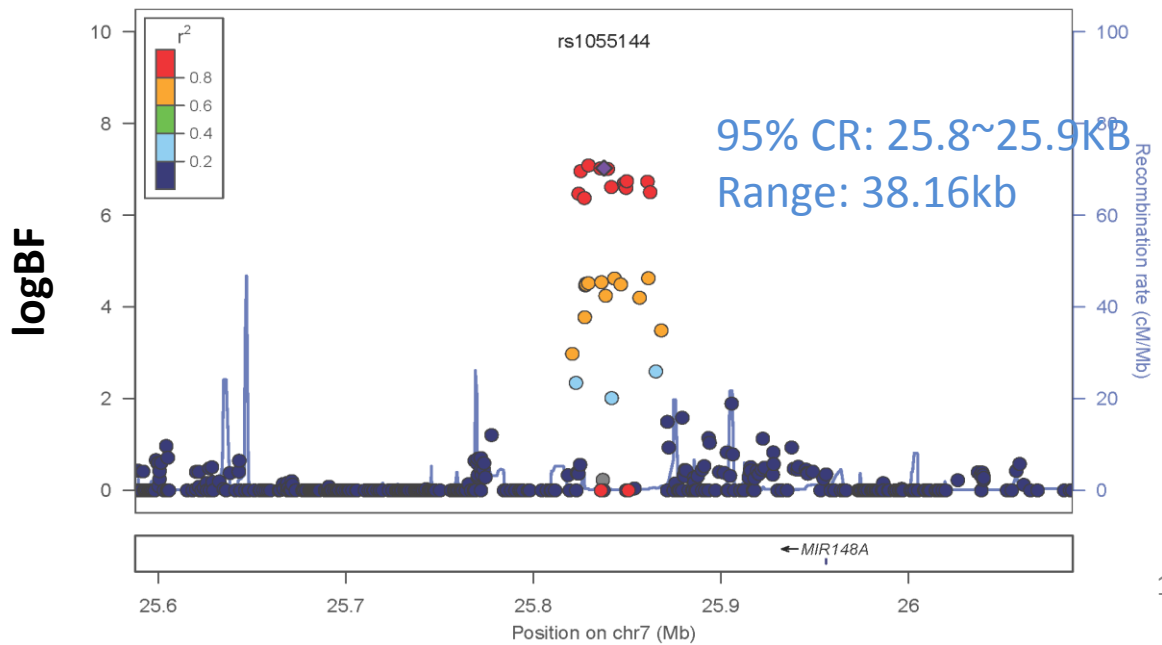
Plotted SNPs

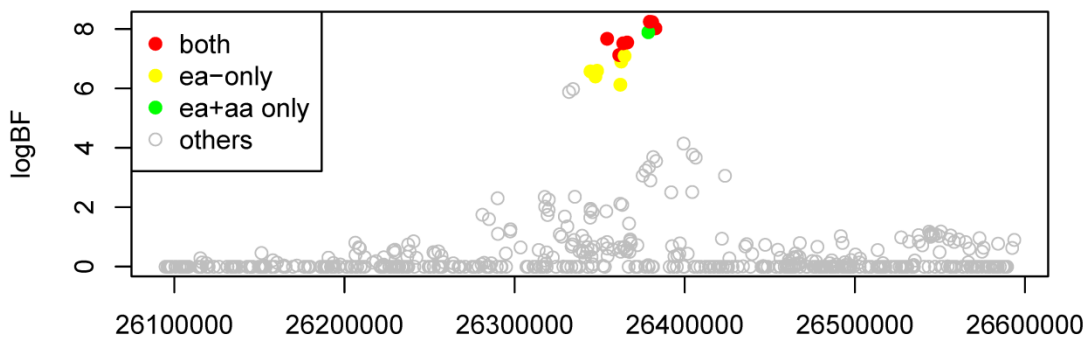
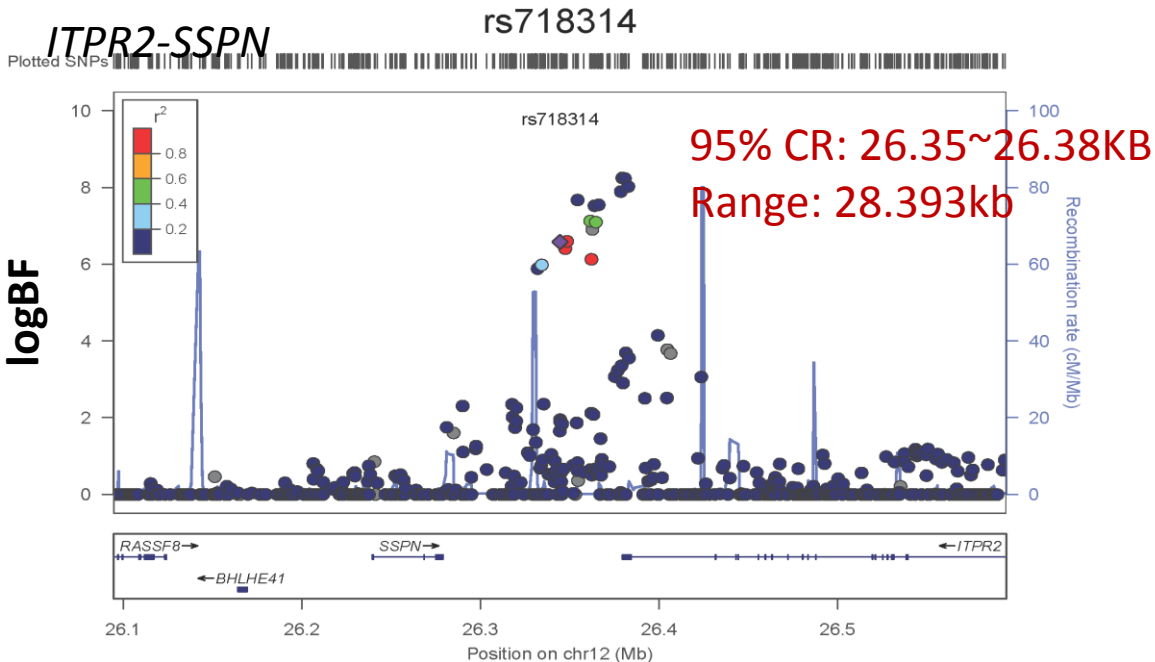


Plotted SNPs

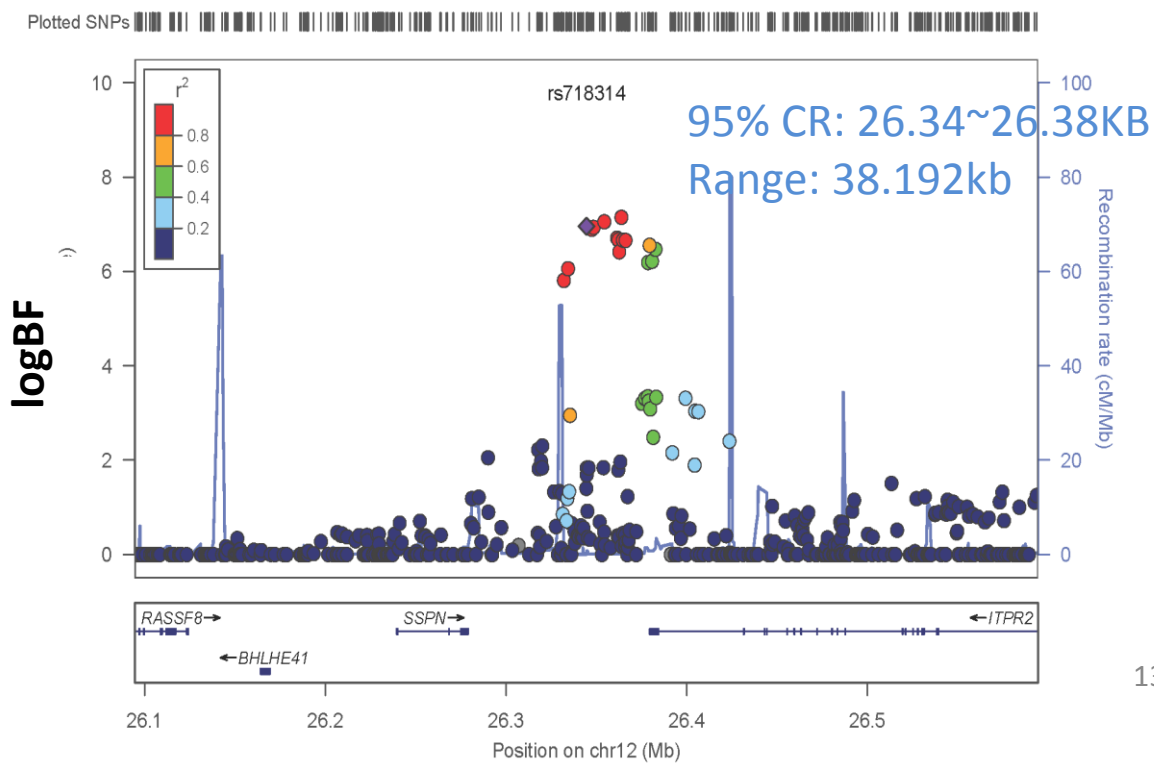


Plotted SNPs



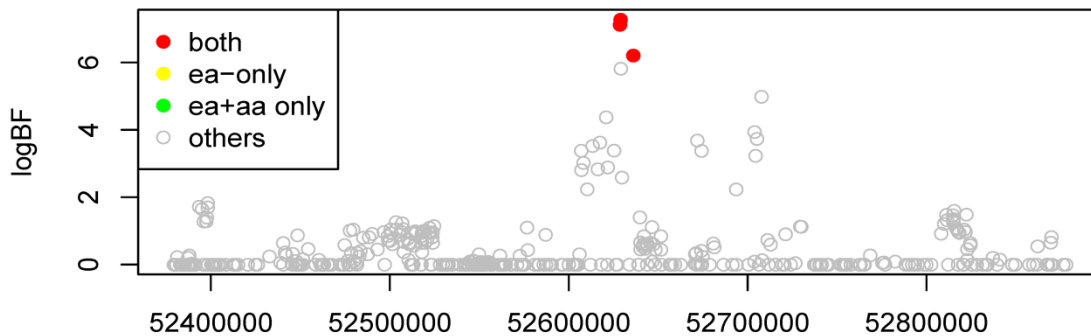
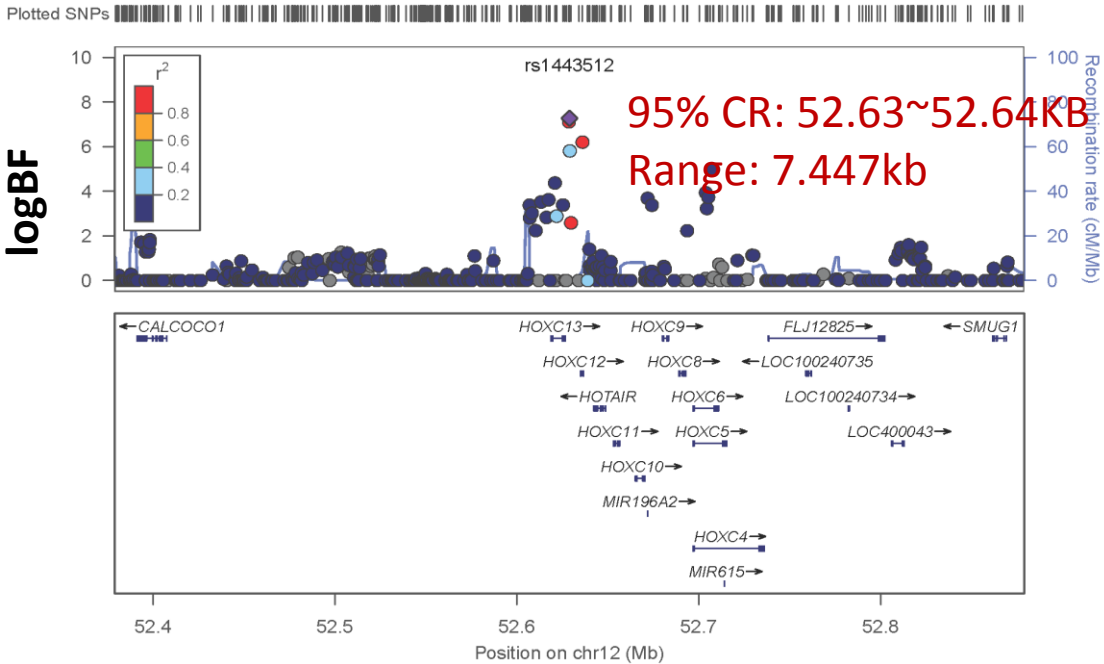


EA Sample Only Result: rs718314

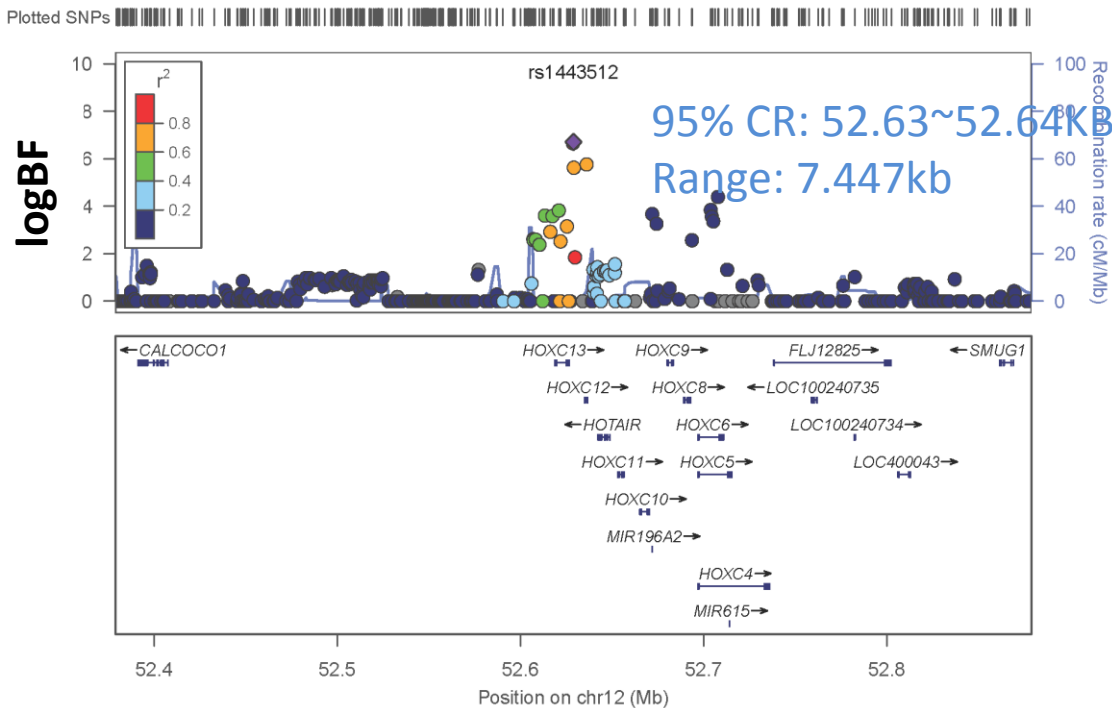


HOXC13

rs1443512



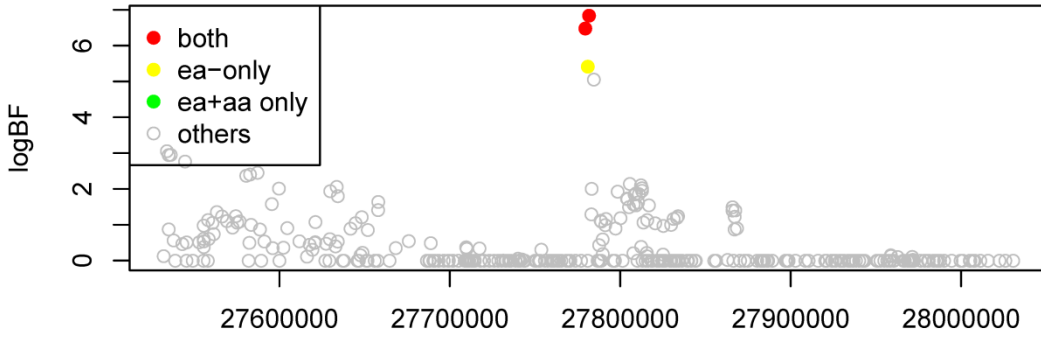
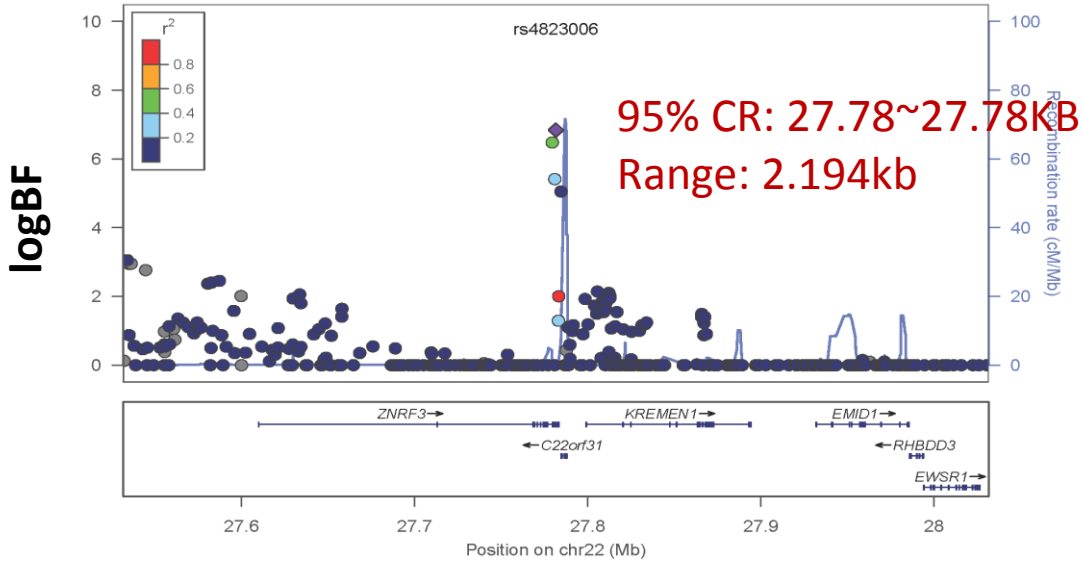
EA Sample Only Result: rs1443512



ZNRF3-KREMEN1

rs4823006

Plotted SNPs



EA Sample Only Result: rs4823006

Plotted SNPs

